U.PORTO

FC FACULDADE DE CIÊNCIAS
UNIVERSIDADE DO PORTO

Improving the Accuracy of Indoor Localization

Marco Augusto de Araújo Primo
Master in Network and Information Systems Engineering
Department of Computer Science
Faculty of Sciences of the University of Porto
2024

Improving the Accuracy of Indoor Localization

Marco Augusto de Araújo Primo
Master in Network and Information Systems Engineering
Department of Computer Science
2024

Supervisor
Prof. Dr. Sérgio Crisóstomo
Faculty of Sciences of the University of Porto

Co-supervisor
Prof. Dr. Rui Prior
Faculty of Sciences of the University of Porto

Acknowledgements

I express my profound gratitude to my wife, Lais. Your unwavering support, understanding, and love have driven my academic journey. Your encouragement, wisdom, and companionship made this path possible and worthwhile. To my parents, my great gratitude. From my first days, you instilled hard work, perseverance, and integrity. Your belief and sacrifices for my education have been the foundation of all my achievements. I am immensely grateful to my professors, Sérgio Crisóstomo and Rui Prior. Their guidance, expertise, and mentorship have shaped this work and my growth as a scholar. I want to thank Instituto de Telecomunicações (UIDB/50008/2020) for hosting this work.

UNIVERSIDADE DO PORTO

Abstract

Faculdade de Ciências da Universidade do Porto
Departamento De Ciência De Computadores

Master in Network Engineering and Computer Systems

Improving the Accuracy of Indoor Localization

by Marco PRIMO

In contemporary society, digital technology is deeply integrated into everyday activities. One notable instance is the pervasive use of smartphones, which facilitate a wide range of functions, including food ordering, navigation, and electronic payments. The core technology enabling many of these capabilities is geolocation systems. The Global Positioning System (GPS) is a prominent geolocation system renowned for its efficacy in most scenarios, delivering satisfactory positional accuracy. However, GPS technology does not suits for scenarios where a centimeter-level precision is needed or when the satellite-to-device line of sight (LOS) is obstructed. In order to overcome such scenarios, a vast lack of alternative technologies have been proposed over the years.

In 2016, the IEEE introduced the 802.11mc protocol, also known as Wi-Fi RTT. This protocol enables access points to respond to ”finite time measurement” (FTM) requests, allowing users to calculate their distance relative to the access point. Thus, the 802.11mc protocol provides a means to leverage existing infrastructure to overcome location-based challenges. Prior to the advent of 802.11mc, Wi-Fi signals were already utilized for location systems, primarily based on signal strength, or RSSI, to construct a ”fingerprint” map. However, due to the dynamic nature of indoor environments, such maps would rapidly become obsolete if not continually updated. Systems incorporating 802.11mc have demonstrated resilience to these issues, although they are not entirely immune.

Similarly, Ultra-Wideband (UWB) has emerged as a robust technology for high-precision localization, surpassing the accuracy of Wi-Fi RTT. UWB operates at higher frequencies and employs time-of-flight measurements to achieve centimeter-level precision, making it particularly suitable for applications such as indoor navigation and object tracking. Its

capability to mitigate interference and provide reliable positioning in complex environments positions UWB as a valuable complement to Wi-Fi RTT in geolocation systems.

This study aims to analyze a potential solution for enhancing the accuracy of location systems that utilize Fine Timing Measurement (FTM). As a byproduct, tools will be developed to facilitate the collection and visualization of FTM data. Additionally, datasets will be generated to support the evaluation of the proposed solution.

UNIVERSIDADE DO PORTO

Resumo

Faculdade de Ciências da Universidade do Porto
Departamento De Ciência De Computadores

Mestrado em Engenharia De Redes e Sistemas Informáticos

Aprimorando a precisão da localização em ambientes internos

por Marco PRIMO

Na sociedade contemporânea, a tecnologia digital está profundamente integrada às atividades cotidianas. Um exemplo notável é o uso disseminado de smartphones, que facilitam uma ampla gama de funções, incluindo pedidos de comida, navegação e pagamentos eletrônicos. A principal tecnologia que possibilita muitas dessas capacidades são os sistemas de geolocalização. O Sistema de Posicionamento Global (GPS) é um sistema de geolocalização proeminente, conhecido por sua eficácia na maioria dos cenários, oferecendo precisão posicional satisfatória. No entanto, a tecnologia GPS pode ser insuficiente em circunstâncias que exigem precisão de nível centimétrico ou quando a linha de visada entre o satélite e o dispositivo é obstruída. Para superar essas limitações, várias tecnologias alternativas foram desenvolvidas ao longo dos anos. Notavelmente, Wi-Fi e Ultra-Wideband (UWB) surgiram como soluções viáveis de posicionamento.,Em 2016, o IEEE introduziu o protocolo 802.11mc, também conhecido como Wi-Fi RTT. Este protocolo permite que pontos de acesso respondam a solicitações de ″medição de tempo finito″ (FTM), permitindo aos usuários calcular sua distância em relação ao ponto de acesso. Assim, o protocolo 802.11mc oferece um meio de aproveitar a infraestrutura já existente para superar desafios baseados em localização. Antes do advento do 802.11mc, os sinais de Wi-Fi já eram utilizados para sistemas de localização, principalmente baseados na intensidade do sinal, ou RSSI, para construir um mapa de ″impressões digitais″. No entanto, devido à natureza dinâmica dos ambientes internos, esses mapas rapidamente se tornariam obsoletos se não fossem atualizados continuamente. Sistemas que incorporam o 802.11mc têm demonstrado resistência a essas questões, embora não sejam totalmente imunes.,Da mesma forma, a Ultra-Wideband (UWB) emergiu como uma tecnologia robusta para localização de alta precisão, superando a precisão do Wi-Fi RTT. A UWB

opera em frequências mais altas e emprega medições de tempo de voo para alcançar precisão de nível centimétrico, tornando-a particularmente adequada para aplicações como navegação interna e rastreamento de objetos. Sua capacidade de mitigar interferências e fornecer posicionamento confiável em ambientes complexos posiciona a UWB como um complemento valioso para o Wi-Fi RTT em sistemas de geolocalização.,Este estudo visa analisar soluções potenciais para melhorar a precisão dos sistemas de localização que utilizam FTM. Duas tecnologias serão avaliadas: tecnologia Ultra-Wideband e 802.11mc, também conhecida como Wi-Fi RTT.

Contents

List of Figures

Chapter 1

Introduction

In the modern era, localization systems have become integral to our daily lives. Location-based services (LBS) are now embedded in a multitude of applications, ranging from navigation systems that help us find our way to tracking personnel and assets and even influencing behavior in leisure and business applications. One of the most significant challenges facing these localization systems is the seamless transition between outdoor and indoor environments.

The Global Navigation Satellite System (GNSS), the most prevalent technology for outdoor localization, struggles to maintain its effectiveness indoors due to inherent characteristics that can weaken or even eliminate the GPS signal, due to the lack of line-of-sight which is a critical principle underlying the functionality of the GNSS; Figure 1.1 illustrates a line-of-sight scenario. Without line of sight, the signal has to pass through building materials like concrete, wood, and metal, and then the signal is attenuated or diminished. Also, signals can reflect off various surfaces like walls, floors, or large metallic objects, resulting in phase interference and erroneous position readings. Consequently, GNSS not being suitable for indoor environments, the need for indoor localization systems has risen.

Unlike outdoor scenarios where GNNS dominates, indoors there is a great diversity of technologies that have been developed or adapted, including WiFi, Bluetooth, Ultra-Wideband (UWB) and Infrared (IR), among others. Each of these technologies has its own strengths and weaknesses, and the choice of technology is primarily dependent on the specific requirements of the application.

Despite the numerous technologies developed for indoor localization, achieving high accuracy and precision remains a significant challenge. Addressing this open problem, this work proposes methodologies to enhance the accuracy of Indoor Localization Systems by capitalizing on the redundant information available within the environment.

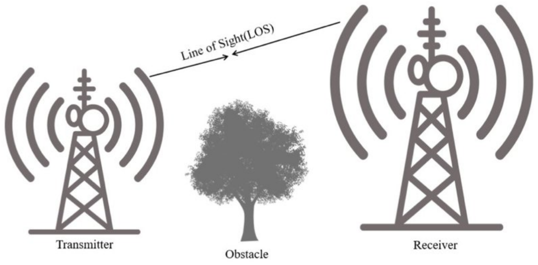

FIGURE 1.1: The figure depicts two communicating devices, labeled Device ”Transmitter” and ”Receiver”, positioned within an outdoor environment. A straight line, labeled ”Line of Sight,” connects the two devices directly, representing the optimal path for wireless signal transmission. This line represents unobstructed propagation, where there are no physical barriers between the devices hindering the signal’s path.[1]

1.1 Hypothesis

Ensuring complete internet access within buildings is a complex task. The challenges involved in providing full coverage depend on the building’s structural complexity. Often, the adopted solution is to deploy multiple access points, resulting in overlapping regions where signals from multiple devices converge. WiFi RTT enables access points to respond to Fine Time Measurement (FTM) requests, given an approximate distance between the receiver and the transmitter. This capability enables the utilization of existing internet access infrastructure for localization purposes.

Taking advantage of this already installed infrastructure, it is possible to translate distances into coordinates without the need for additional equipment. The only restriction is to have the minimum number of transmitter signals reaching the receiver at the point you want to locate. However, it is common in indoor scenarios to simultaneously receive signals from more than the minimum required. This study explores the relationship between the number of FTM responders used in location computation and its impact on accuracy improvement.

1.2 Aims and Objectives

The primary objective of this research is to evaluate how accuracy improves when using more than the minimum required number of Fine Timing Measurement (FTM) responders to determine a location. In a 3D context, at least four distance measurements from different sources are necessary for accurate positioning. However, real-world measurements often contain errors that contribute to inaccuracies. This study investigates the effect of incorporating more than four distance measurements into location computation.

As secondary objectives, this research introduces user-friendly visualization tools and efficient data collection processes, ensuring accessibility for a wider audience. Additionally, it aims to enhance academic resources by providing datasets related to Fine Timing Measurement (FTM) using IEEE 802.11mc and Ultra-Wideband (UWB) technologies.

1.3 Thesis Structure

This thesis is structured into several comprehensive chapters organized as follows:

Chapter 2: Techniques and Technologies delves into the realm of Indoor Positioning Systems (IPS), elucidating the primary techniques and technologies employed to precisely determine the coordinates of a device.

Chapter 3: Related Work stands as a review of the ongoing development and existing research in the field, offering valuable insights into related endeavors and their significance.

Chapter 4: Collection and Data Exploration delineates the process of data gathering and the initial insights derived from it. It details the creation of a dataset and the development of software applications necessary for data collection. The chapter also outlines the challenges encountered during this phase.

Chapter 5: Data Analysis focuses on analyzing the collected data, specifically discussing bias detection through ground truth and calculated distance correlation, offering a critical assessment to further the field of indoor localization.

Chapter 6: Proposed Solutions This chapter elaborates on the conceptual framework and design of the solutions, providing detailed insights into its expected impact and benefits.

Chapter 7: Solution Analysis delves deeper into the analytical aspects of the proposed solutions, evaluating its performance, advantage, and efficiency.

Lastly, **Chapter 8: Conclusion** summarizes the entire study and summarizes the key findings and contributions of the thesis. This final chapter also discusses potential future directions of research, highlighting avenues for further exploration and development in the field of indoor localization.

Chapter 2

Technology and Techniques

The field of indoor localization has seen significant advancements over the past few decades, driven by the increasing demand for precise and reliable location-based services within indoor environments. Unlike outdoor localization, which has been largely addressed by Global Positioning System (GPS) technology, indoor localization presents unique challenges due to the complex nature of indoor environments. These challenges include signal attenuation, multipath propagation, and environmental dynamics.

This chapter aims to provide an overview of related work in indoor localization, exploring the latest advances, methodologies, and technologies developed.

2.1 Indoor Positioning Systems

Indoor Positioning Systems (IPS) are used to locate objects or people inside a building using radio waves, magnetic fields, acoustic signals, or other sensory information collected by mobile devices. They are like indoor GPS, with a variety of use cases such as asset tracking, personnel tracking, etc. Asset tracking can be used to locate equipment, inventory, or vehicles within a large facility. In personnel tracking, it can be used to locate individuals within a building for safety or security purposes.

IPS can also be used in navigation applications to help individuals navigate large buildings such as malls, hospitals, and airports. This can be particularly useful for people with visual impairments.

One of the key challenges in IPS is achieving high accuracy, due to multipath propagation and signal attenuation. In addition to the technical challenges, there are also privacy concerns. Since IPS can track the movement of individuals within a building, there are concerns about the misuse of this information.

Despite all the challenges, the demand for IPS is expected to grow in the coming years due to the increasing need for indoor navigation and the growth of the Internet of Things (IoT). With the advancement of technology and the increasing awareness of privacy, it is expected that the future IPS will be more accurate, reliable, and friendly to privacy.

2.2 Techniques

The realm of positioning is rich with diverse techniques, each suited to various applications and technologies. This section aims to provide an overview of these techniques, detailing their characteristics. The techniques explored are listed below and are applicable to a wide range of technologies.

- Angle of Arrival 2.2.1
- Phase of Arrival 2.2.2
- Time of Flight 2.2.3
- Time Difference of Arrival 2.2.4
- Received Signal Strength Indicator 2.2.5

2.2.1 Angle of Arrival

Angle of arrival (AoA) is a technique that estimates the direction of propagation of a signal by measuring its angle of arrival on a matrix of sensors [2]. To determine the direction from which a signal arrives, specialized hardware is necessary, such as antenna arrays, RF front-ends, analog-to-digital converters, and dedicated signal processing units. These components work together to receive and process signals, convert them into digital form, and apply advanced algorithms to estimate the angle of arrival. Due to the complexity and customization required, implementing AoA typically involves designing or using specialized hardware tailored to the specific application, making it a more complex process than simply connecting a device and expecting it to function seamlessly. [3]. In a localization system based on the angle of arrival (AoA), the location of a tagged device is pinpointed by finding where pairs of imaginary signal paths, defined by their respective angles, intersect. As shown in Figure 2.1.

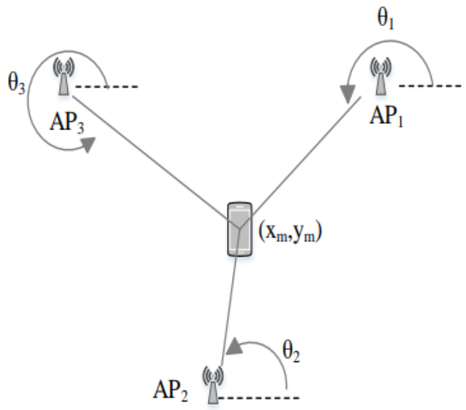

FIGURE 2.1: Localization based on angle of arrival (AoA) measurement [4]

2.2.2 Phase of Arrival

Phase of Arrival (PoA) methods figure out how far apart a sender and receiver are by looking at the phase, which is the position of a wave in its cycle, of the signal they are using. The basic idea is to think of the signals as smooth waves with the same frequency and starting point. To find out the distance between the sender and the receiver, one way is to think about the time it takes for the signal to travel, which is a part of how long the wave is. If you have several antennas, they will each get the signal at a slightly different time, creating a phase difference [5]. This difference can help pinpoint the location of the sender, as you can see in Figure 2.2. A more detailed discussion can be found at [6].

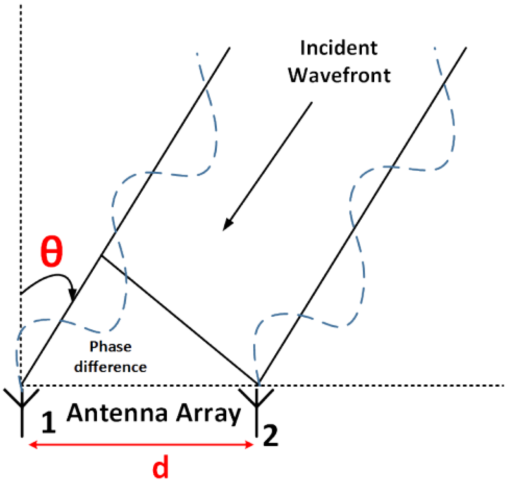

FIGURE 2.2: PoA based localization [5]

2.2.3 Time of Flight

The Time of Flight (ToF) technique is a method used in various applications to measure the distance between a sensor and an object. It works by calculating the time it takes for a signal, often a light pulse or radio wave, to travel from the sensor to the object and back again [5]. It is crucial to understand that the receiving stations need extremely precise timing mechanisms. Even a tiny timing error of just one microsecond (1 µs) in estimating the delay can lead to a substantial distance estimation error. The distance between the two actors is estimated using the following equation [7]:

$$d = (t_i - t_0) \times c \tag{2.1}$$

where t0 and ti are the instant of signal transmission and reception time, respectively, and c = 3 × 108 m/s, the speed of light

The simplicity and hardware compatibility make ToF a more straightforward and accessible technique compared to others, as it can be implemented without the need for specific hardware configurations or additional components.

The precision of Time-of-Flight (ToF) measurements hinges on the signal's bandwidth and its sampling rate. A higher bandwidth can improve the system's ability to resolve small differences in ToF, while a higher sampling rate ensures that the signals are captured with sufficient granularity, reducing the risk of missing the exact arrival time due to infrequent measurements [5]. However, despite advances such as increased bandwidth and super-resolution techniques that bolster ToF performance, these improvements cannot completely offset significant localization errors that arise when there is no direct line of sight between the transmitter and receiver. Obstructions in the direct path can lead to multipath propagation issues, which remain a challenge for accurate ToF-based localization. A specialized version of ToF is the Round Trip Time of Flight RToF which eliminates the necessity to have a synchronized clock between devices.

2.2.4 Time Difference of Arrival

For measuring the time difference between arrivals (TDoA), it is necessary to look at the difference in the time it takes for a signal to reach different access points (AP). The TDoA localization determines how much closer or farther the device is from these receivers by checking these time differences.

$$d_{ij} = (t_i - t_j)c = \sqrt{(x_i - x_m)^2 + (y_i - y_m)^2} - \sqrt{(x_j - x_m)^2 + (y_j - y_m)^2} \tag{2.2}$$

Equation 2.2 defines d_{ij} as the distance difference for a signal to travel from two receivers, labeled i and j, to a device, determined by the Time Difference of Arrival (TDOA) method [8]:

- d_{ij} is the difference in distance to the device from receiver i and receiver j.
- t_i and t_j are the times of signal reception at the device from receiver i and receiver j, respectively.
- c is the speed of light, used for converting time difference into distance.
- The square root terms calculate the Euclidean distances from the device to each receiver using their coordinates (x_i, y_i) and (x_j, y_j), with (x_m, y_m) being the coordinates of the device.

The equation computes the difference between the distances to the receivers i and the AP j of a device. Geometrically, this forms a hyperboloid when plotted in a three-dimensional space. TDOA localization techniques utilize these measurements from multiple receivers to triangulate the precise location of the device. The accuracy of this method depends on the precise timing and synchronization between the receivers.

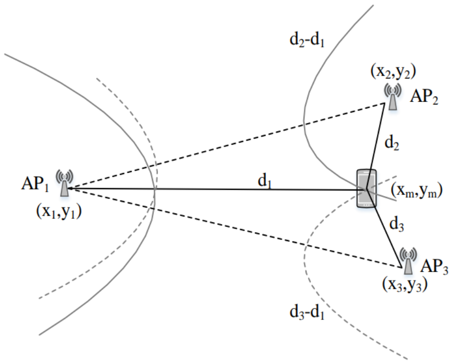

FIGURE 2.3: Localization based on time difference of arrival (TDOA) measurement [4]

2.2.5 Received Signal Strength Indicator

RSSI (Received Signal Strength Indicator) is another technique that, similar to Time of Arrival (ToA), is highly accessible and does not require specialized hardware. RSSI is a metric used to quantify the strength of the received signal in a receiver[9]. It is typically measured in decibels (dB) and can provide valuable information about the signal power level. The accessibility makes RSSI and ToA popular choices for IPS.

2.3 Technologies

To have a functional and effective indoor positioning system (IPS), it is essential to carefully evaluate various factors, including the chosen technology and the corresponding techniques. The type of technology selected for the IPS inherently determines the range of applicable techniques. Additionally, each technology comes with its own set of tradeoffs, which must be thoroughly considered. The subsequent sections of this chapter are dedicated to examining and categorizing the technologies and techniques that apply to the development of an IPS.

2.3.1 Ultra-Wideband (UWB)

Ultra-wideband (UWB) technology, known for its large bandwidth (>500MHz) and ultra short-pulses with a period of <1 nanosecond (ns), is very attractive for indoor localization by offering precise and reliable tracking information. These benefits stem from the inherent immunity of UWB to interference from other signals, due to its distinct signal type and the use of a broad radio spectrum. Moreover, UWB signals possess the remarkable ability to penetrate various construction materials with ease. This technology is unique in various industries, including logistics, healthcare and manufacturing, due to its accuracy at the centimeter level and its low power consumption [10, 11]. However, to ensure minimal interference with other devices, UWB applications must operate within specific short frequency ranges, despite the wide frequency range of the UWB [12].

The prevalent technique associated with Ultra-Wideband (UWB) technology often revolves around Time of Flight (ToF) 2.2.3.

2.3.2 Light Detection and Ranging

Light Detection and Ranging (LiDAR) is a remote sensing method that uses light in the form of a pulsed laser to measure distances. Provides detailed information about the contours of the surrounding obstacles. When combined with inertial sensors, it can offer accurate localization[3, 13]. LiDAR measures distance by emitting focused pulses of laser

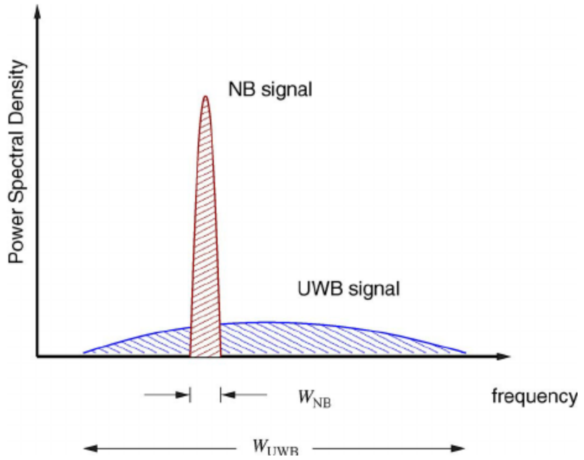

FIGURE 2.4: Power spectral density of UWB and NB signals [11]

light toward a target and then measuring the time it takes for each pulse to bounce back, a technique known as time of flight (ToF) 2.2.3. This technology offers high precision in measuring distances, yet this comes at a higher financial cost compared to other technologies, Figure 2.5 describes the process of surface mapping, in which an aircraft equipped with laser ranging technology flies over the terrain. This method involves emitting laser beams toward the surface measuring the time it takes for the light to bounce back to the aircraft. The distance is further calculated using $d = \frac{C \times T}{2}$, where C is the speed of light constant and T is the time it takes for the laser to travel from the source to the target.

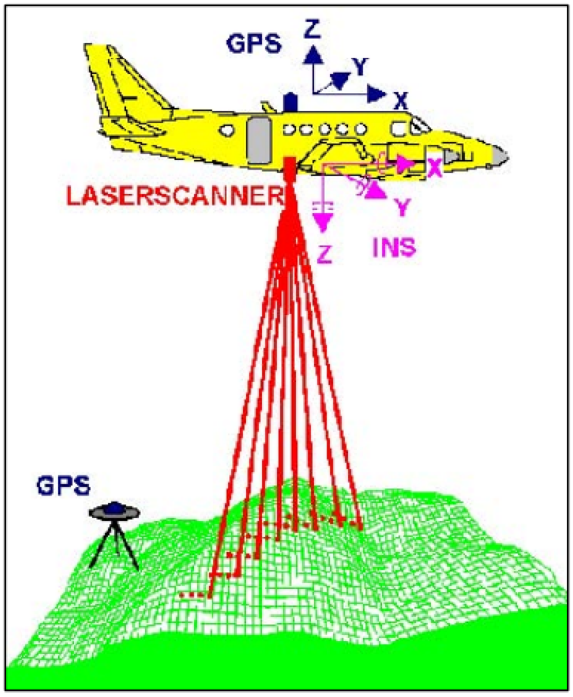

FIGURE 2.5: Basic lidar data collection schematic from aircraft [14]

2.3.3 Bluetooth Low Energy

Bluetooth Low Energy (BLE), also referred to as Bluetooth Smart, offers significant improvements over older versions, boasting a data rate of 24Mbps and a coverage range of 70-100 meters, while maintaining a higher energy efficiency [9]. Although BLE is compatible with various localization techniques such as the Received Signal Strength Indicator (RSSI) [9], Angle of Arrival (AoA) [2], and Time of Flight (ToF) 2.2.3, most existing BLE-based localization solutions predominantly rely on RSS-based inputs due to their simplicity. However, Receiver Signal Strength (RSS) is challenging to use because environmental changes directly affect the measurements, often resulting in inaccurate localization. Despite this limitation, BLE, with its range, cost-effectiveness, and energy efficiency attributes, serves as a viable option for localization. Notably, two BLE-based protocols have emerged, i.e., iBeacons (by Apple Inc.) and Eddystone (by Google Inc.), primarily focusing on context-aware proximity-based services.

The working principle of IPS based on BLE is the use of tags to determine the Received Signal Strength (RSS) from surrounding BLE beacons by capturing the beacons' broadcasted advertisement packets. These packets are typically transmitted at intervals varying between 100 and 2000 milliseconds. For Indoor Positioning Systems (IPS), BLE beacons are commonly set to broadcast at an interval of approximately 300 milliseconds, a setting chosen based on the average human walking speed of 1.3 meters per second. Furthermore, the frequency at which these signals are scanned can be configured in the positioning application, with a typical scanning interval of about 1000 milliseconds (1 second), enabling the generation of positioning information per second[4]. Figure 2.6 illustrates a typical BLE-based IPS architecture.

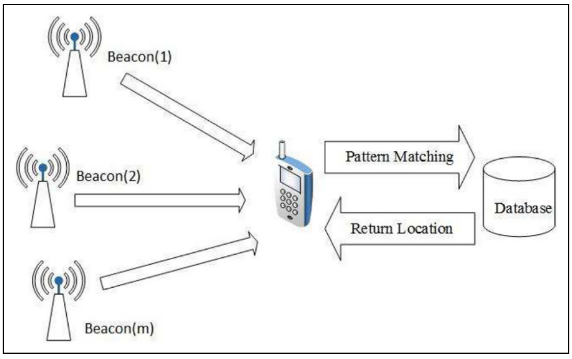

FIGURE 2.6: System architecture of the Bluetooth positioning system[15]

2.3.4 Wi-Fi

Wi-Fi-based indoor positioning systems leverage the existing Wi-Fi infrastructure to provide indoor localization, which makes this technology very attractive for building IPS, since the deployment cost will be zero, which makes WiFi an ideal candidate for indoor localization and one of the most widely studied localization technologies in the literature. These systems mainly employ techniques such as Received Signal Strength Indication (RSSI) 2.2.5 or Time of Flight (ToF) 2.2.3 measurements to estimate the distance between the Wi-Fi access point and the device to be located[3].

A notable advancement in Wi-Fi-based indoor positioning is the introduction of Wi-Fi Round Trip Time (RTT), also known as 802.11mc. The support for Wi-Fi RTT on Android smartphones was introduced in Android 9 (Pie) [16] which allows an Android device to calculate the distance to a Wi-Fi access point and determine its indoor position with an accuracy of 1-2 meters [16]. Wi-Fi RTT works by measuring the trip time of a signal between the device and the Wi-Fi access point[17]. The working principle is depicted in Figure 2.10, where the distance between the receiver and the transmitter is obtained knowing the time it takes for the signal to travel back and forth. However, determining the round trip time (RTT) for WiFi signals poses a challenge due to the lack of synchronization between internal clocks in real-world scenarios, where the actors will be smartphones and access points most of the time. Although one-way time measurements based on timestamp differences are not feasible, a clever approach leverages reverse signal travel. Taking into account the differences in timestamps during both forward and reverse signal propagation, the RTT can be accurately calculated without requiring knowledge of clock offsets, as shown in the equation below [18].

$$d = \frac{c \cdot (t_4 - t_1) - (t_3 - t_2)}{2}$$

In the equation of distance calculation using RTT it is considered four timestamps.

1. **T_1** The moment the signal departs from the WiFi access point (AP).
2. **T_2** The instant the signal arrives at the smartphone (STA).
3. **T_3** The time that the signal leaves the smartphone (STA) for its return journey.
4. **T_4** The point at which the signal reaches the AP again.

The difference between (T_4 - T_1) corresponds to the total time taken for the signal to travel from the AP to the smartphone and back. Similarly, (T_2 - T_3) represents the time for the reverse journey.

To calculate the RTT, it is necessary to multiply the difference in timestamps by the speed of light constant, which approximates the velocity of the signal. However, there is a crucial consideration: The difference represents the distance traveled from the smartphone to the access point and from the access point to the smartphone. To obtain the distance between the smartphone and the access point, it is necessary to divide this value by two.

In summary, the RTT is determined by combining these forward and reverse signal travel times, accounting for the speed of light, and adjusting for the two-way journey.

Wi-Fi RTT or 802.11mc represents a significant step forward in the field of Wi-Fi-based indoor positioning, offering improved accuracy and reliability. It opens up new possibilities for indoor navigation, location-based services, and even augmented reality applications.

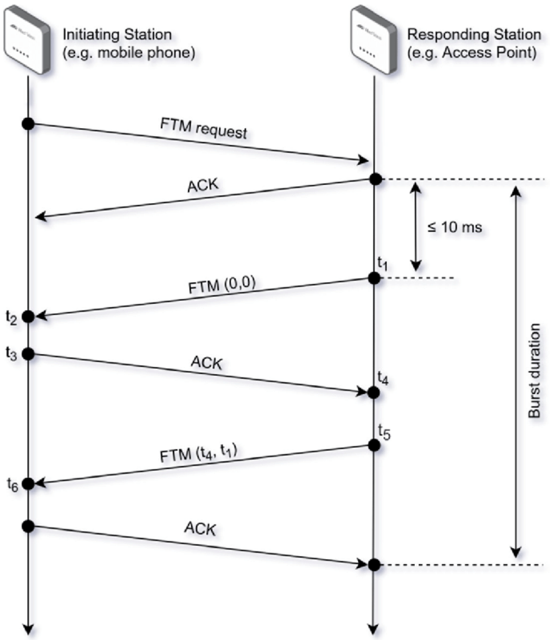

FIGURE 2.7: Basic procedure to gather round-trip-time RTT measurements in IEEE-80211mc [19]

2.3.5 Radio Frequency Identification (RFID)

RFID technology is primarily designed for the seamless transfer and storage of data via electromagnetic transmission, allowing communication between a transmitter and any radio frequency (RF) compatible circuit[3] [20]. An RFID system consists of a reader that can communicate with RFID tags. The RFID tags emit data that the RFID reader can read using a predefined RF and protocol, known to both the reader and tags a priori. There are two types of RFID

1. **Active RFIDs** operate within the Ultra High Frequency (UHF) and microwave frequency range. These RFIDs are powered by a local power source and periodically transmit their ID. They can operate at distances of hundreds of meters from the RFID reader. Active RFIDs are commonly used for localization and object tracking due to their reasonable range, cost effectiveness, and ease of embedding into tracking objects. However, they typically cannot achieve submeter accuracy and are not readily available on most portable user devices.

2. **Passive RFIDs** operates within a limited communication range, typically around 1-2 meters, and do not require a battery for operation. These RFID tags are smaller, lighter, and more cost effective compared to active ones. They can operate on a wide range of frequencies, including low, high, UHF, and microwave frequencies. While passive RFIDs offer an alternative to barcodes, especially when the tag is not within the reader's line of sight, their limited range makes them unsuitable for indoor localization. However, they can be utilized for proximity-based services through brute-force approaches. However, implementing such services would require modifications to the existing passive RFID procedures, such as transmitting an ID for identification purposes.

2.3.6 Visible Light Communication

Visible Light Communication (VLC) is an emerging technology renowned for its high-speed data transfer capabilities [21–23]. It operates within the visible-light spectrum, typically between 400 and 800 terahertz (THz), utilizing modulation techniques emitted primarily by light-emitting diodes (LEDs). Localization techniques based on visible light employ light sensors to precisely measure the position and direction of the LED emitters. In essence, the LEDs, functioning similar to iBeacons, transmit signals that receivers/sensors can capture for localization purposes. Among these techniques, the angle of arrival (AoA) is regarded as particularly accurate [21]. One significant advantage of visible-light-based localization lies in its widespread adoption, potentially exceeding even WiFi. However, a critical constraint is the need for a direct line of sight between the LED and the sensor(s) for precise localization. However, this constraint is the reason why the VLC is so robust against multipath distortion, resulting in more stable and predictable signal propagation. The growing prevalence of LED technology furthers the case for VLC systems using such technology, such systems can provide extensive coverage offering uninterrupted service over a much wider area than current positioning technologies [23].

2.3.7 Sound-Based Technologies

Sound-based Indoor Positioning Systems (IPS) can be implemented using two primary methods: ultrasonic and acoustic. In both cases, the predominant technique employed is Time-of-Flight (ToF), as referenced in Section 2.2.3. This approach, one of the earliest in the realm of localization, remains in use because of its effectiveness.

However, sound-based IPS have notable limitations, primarily their vulnerability to environmental noise. This is a significant challenge in indoor settings, where sound from various sources often interferes with the IPS. Additionally, these systems are affected by multipath propagation, where sound waves reflect off surfaces, leading to signal distortion and inaccuracies in localization.

In sound-based systems, where the speed of sound is significantly slower than the speed of light, there is less demand for stringent processing requirements, then the appeal for sound-based IPS lies in their cost-effectiveness[3].

Moreover, the concept of using sound for localization is not limited to technological applications. In the animal kingdom, numerous species use sound for navigation and locating objects. This fascinating aspect of animal behavior demonstrates the versatility and significance of sound as a navigational tool in different domains [3].

2.4 Methods

Indoor positioning systems (IPS) rely on a variety of methods to estimate the location of a device within an indoor environment. These methods use data from different technologies, such as Wi-Fi signals, BLE, and inertial sensors, to estimate a device's location. This section aims to review the most widely deployed methods that address indoor localization.

2.4.1 MultiLateration

Multilateration is a method used to determine the position of an object based on measurements of the distance to at least three known points [24]. The mathematical principle behind multilateration in its simplest form is based on the properties of circles. Given three points A, B, and C with known coordinates, and the distances d_A, d_B, and d_C from an unknown point P to these points, the position of P can be determined by solving the following equation system:

$$\begin{aligned}
(x - x_A)^2 + (y - y_A)^2 &= d_A^2, \\
(x - x_B)^2 + (y - y_B)^2 &= d_B^2, \\
(x - x_C)^2 + (y - y_C)^2 &= d_C^2.
\end{aligned}$$

These equations represent the equations of the circle in two-dimensional space, with A, B, and C as the centers and d_A, d_B, and d_C as the radii [25]. The solution to this system of equations is the coordinates of the point P, which is the intersection of these three spheres.

However, the above approach relies on accurate distance measurements to determine the position of an object. In real-world applications, these measurements often contain noise due to various factors such as signal interference, atmospheric conditions, and hardware limitations. This noise can significantly affect the accuracy of the multilateration process.

The presence of noise in distance measurements introduces uncertainty in the calculated position of the object. This noise in the distance measurements translates into uncertainty in the radii of the spheres in the system of equations. This means that instead of intersecting at a single point, the intersection will be a region as illustrated in Figure 2.8. In order to work around the possibility of having noise in the distance measurements a specialized multilateration technique can be applied. Instead of relying on solving equations to find the target location, it may be worth trying to find the point that minimizes the error in the location of the target device. The gradient descent algorithm is one algorithm to perform such a minimization task. The versatility of gradient descent lies in its ability

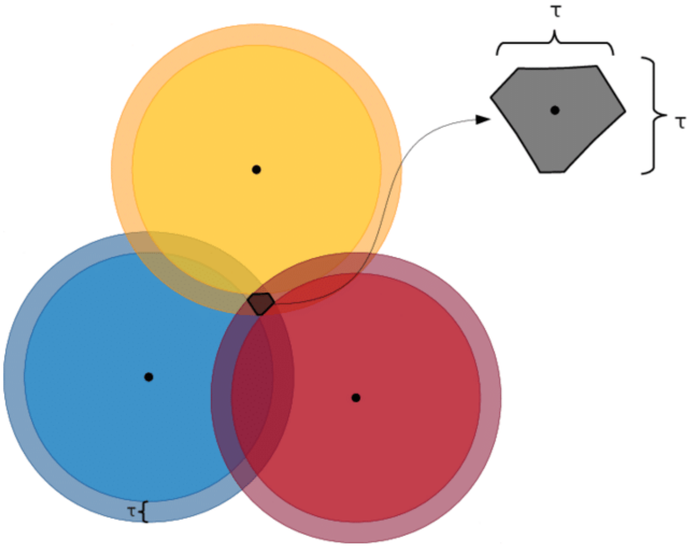

FIGURE 2.8: Trilateration problem where the measurements contain noise and the intersection of the circles is an area [26]

to adapt the cost function based on the type of measurement being used. In the following sections, we will focus primarily on distance measurements to delve deeper into the workings of the gradient descent algorithm[27].

2.4.2 Triangulation

Triangulation is an algorithm that uses the angles formed between the device and at least three known points to calculate the unknown location [28].

The principle behind triangulation is straightforward. Imagine a device within an indoor environment that can detect signals from three different access points. If the device can measure the angle between its line of sight and each access point, and if the distances between the access points are known, then the exact location of the device within the environment can be determined [29]. This is the essence of triangulation.

Despite its simplicity, triangulation is a powerful tool with a wide range of applications in indoor localization. However, it also has its limitations. For example, the accuracy of triangulation can be affected by factors such as signal interference and multipath propagation. Therefore, it is often used in combination with other techniques, such as trilateration and fingerprinting, to improve the accuracy and reliability of indoor localization systems.

2.4.3 Fingerprinting

Fingerprinting is a popular algorithm used in indoor localization systems that use RSSI techniques. It involves creating a map of signal strengths, or a ”fingerprint,” of an environment, and then comparing a device’s current signal strengths to this map to estimate its location. When used with Received Signal Strength Indicator (RSSI) values from wireless signals, this technique can provide accurate location estimates even in complex environments [30].

The principle behind fingerprinting is straightforward. It has two phases, an offline and an online phase. During an offline phase, the indoor environment is divided into a grid of cells and the RSSI values from multiple access points (e.g., Wi-Fi access points or Bluetooth beacons) are measured at each cell. These measurements are then stored in a database, creating a ”fingerprint” of the environment.

During the online phase, the device measures the RSSI values from the access points and compares these measurements to the fingerprints in the database. The location of the device is then estimated to be the cell with the most similar fingerprint.

2.4.4 Machine Learning

Machine learning methods are a class that can learn patterns from data and make predictions based on these patterns [31]. In the context of indoor localization, machine learning can be used to learn the relationship between measurement values and then use this relationship to estimate the position of the device based on new measurements [32].

There are many different types of machine learning algorithms, each with its own strengths and weaknesses. Some of the most commonly used algorithms for indoor localization include k closest neighbors, support vector machines, and neural networks.

Each of these algorithms works in a slightly different way, but they all involve learning a model from a set of training data and then using this model to make predictions. The precision of these predictions depends on the quality of the training data and the suitability of the algorithm to the environment.

Machine learning algorithms can be broadly classified into three categories: supervised learning, unsupervised learning, and reinforcement learning.

- **Supervised Learning**: In supervised learning, the model is trained on a labeled dataset, i.e., a dataset that includes both the input data and the corresponding correct output. The goal of the model is to learn a mapping from inputs to outputs that can be used to make predictions on new, unseen data. Examples of supervised learning algorithms include linear regression, decision trees, and support vector machines [33].
- **Unsupervised Learning**: In unsupervised learning, the model is trained on an unlabeled dataset, i.e., a dataset that includes only the input data. The goal of the model is to learn the underlying structure of the data or to find patterns in the data. Examples of unsupervised learning algorithms include clustering algorithms and dimensionality reduction algorithms [34].
- **Reinforcement Learning**: In reinforcement learning, the model learns to make decisions by interacting with an environment. The model receives feedback in the form of rewards or penalties, and its goal is to learn a policy that maximizes the total reward over time. Examples of reinforcement learning algorithms include Q-learning and policy gradient methods [35].

2.5 Iterative Methods

Section 2.4, describes methods that are capable of transforming a one-shot time window of measurements into locations. This section aims to detail methods that require a larger time window to output a fine location.

2.5.1 Gradient descent

The gradient descent algorithm works by iteratively adjusting the estimated position to minimize the cost function, which is, in the case of distance measurements, the sum of the error between the measured distances and the calculated distance using the guess position. The algorithm can be summarized as follows [36] [37]:

1. Initialize the estimated position.
2. Compute all the distances between the AP and the mobile device.
3. Update the estimated position based on the calculated error and the gradient of the cost function.

4. Repeat steps 2 and 3 until the cost function is minimized or a predetermined number of iterations has been reached.

The cost function is defined as:

$$E(\mathbf{r}) = \sum_{i=1}^{N} \left(\|\mathbf{r} - \mathbf{r}_i\| - d_i \right)^2 \tag{2.3}$$

where $\mathbf{r}$ is the estimated position, $\mathbf{r}_i$ is the position of the i-th known point, d_i is the measured distance to the i-th point, and N is the total number of known points.

In this case, we want to find the position $\mathbf{r}$ that minimizes the cost function $E(\mathbf{r})$. The cost function gradient gives the direction of the steepest ascent, and so by moving in the opposite direction we can iteratively adjust the estimated position to reduce the cost.

$$\mathbf{r}_{n+1} = \mathbf{r}_n - \gamma \nabla E(\mathbf{r}_n) \tag{2.4}$$

where $\nabla E(\mathbf{r}_n)$ is the cost function gradient in the n -th iteration, γ is a step size parameter, and $\mathbf{r}_{n+1}$ is the updated position.

The cost function gradient is given by the following.

$$\nabla E(\mathbf{r}) = 2 \sum_{i=1}^{N} \left(\|\mathbf{r} - \mathbf{r}_i\| - d_i \right) \frac{\mathbf{r} - \mathbf{r}_i}{\|\mathbf{r} - \mathbf{r}_i\|} \tag{2.5}$$

2.5.2 Kalman Filtering

The Kalman Filter is a recursive algorithm estimator that provides a mathematical technique to estimate the state of a process, in a way that minimizes the mean of the squared error. It is optimal for systems that are linear and Gaussian [38].

In indoor localization, the Kalman Filter can be used to estimate the position and velocity of an object based on a series of measurements over time. It works by predicting the next state of the object based on the current estimate and the motion model, and then updating this prediction when a new measurement is received. The Kalman Filter is particularly effective when the noise in the motion and measurement models is Gaussian and the models themselves are linear, but it can also be extended to handle non-linear models through techniques such as the extended Kalman Filter or the unscented Kalman Filter [39].

The Kalman filter operates in two steps: prediction and update [40].

1. **Prediction**: In this step, the filter predicts the current state of the system based on the previous state. This is done using the state transition model. If we denote the state at time k as x_k and the state at time $k-1$ as x_{k-1}, the prediction step can be represented as:

   $$x_k^- = F_k x_{k-1} \tag{2.6}$$

   where F_k is the state transition model which is applied to the previous state x_{k-1}. The superscript ”-” denotes a prediction.

2. **Update**: In this step, the filter updates the predicted state by incorporating the new measurement. This is done using the measurement model. If we denote the measurement at time k as z_k, the update step can be represented as:

   $$x_k = x_k^- + K_k(z_k - H_k x_k^-) \tag{2.7}$$

   where H_k is the measurement model that is applied to the predicted state x_k^-, z_k is the actual measurement and K_k is the Kalman gain.

These two steps are repeated for each time step, allowing the filter to adapt to changes in the system over time. The Kalman filter, as already mentioned, is particularly effective in situations where the system is linear and the noise is Gaussian. However, it can also be adapted to handle non-linear systems and non-Gaussian noise.

2.5.3 Particle Filtering

The Particle Filter, also known as the Sequential Monte Carlo method, is a nonparametric implementation of the Bayes filter. It represents the posterior density function by a set of random samples (particles) with associated weights and uses these to approximate the true state of a system [41].

In the context of indoor localization, each particle represents a potential position of the object being tracked. The particles are propagated over time according to a motion model, and their weights are updated based on the likelihood of the observed measurements given the state of the particles. This allows the Particle Filter to handle non-linear and non-Gaussian problems, which are common in indoor localization due to the complex propagation of signals in indoor environments.

The main idea behind particle filtering is to represent the posterior distribution of the state by a set of random samples, or particles, and to compute estimates based on these samples. Each particle represents a possible state of the system and has a weight associated with it that represents the probability of that state given the observations.

The particle filter operates in two main steps: prediction and update [42].

1. **Prediction**: In this step, the filter propagates each particle from the previous time step forward in time according to the system dynamics. This is typically done by sampling from the system's transition model. If we denote the state of the i-th particle at time k as $x_k^{(i)}$, and the state transition model as f, the prediction step can be represented as:

$$x_k^{(i)} = f(x_{k-1}^{(i)}, u_k, w_k^{(i)}) \tag{2.8}$$

   where u_k is the control input at time k, and $w_k^{(i)}$ is the process noise for the i-th particle at time k.

2. **Update**: In this step, the filter updates the weights of the particles based on the new observation. This is typically done by evaluating the observation model at the predicted state of each particle. If we denote the observation at time k as z_k, and the observation model as h, the update step can be represented as:

$$w_k^{(i)} = w_{k-1}^{(i)} \cdot h(z_k, x_k^{(i)}, v_k^{(i)}) \tag{2.9}$$

   where $v_k^{(i)}$ is the observation noise for the i-th particle at time k. The weights are then normalized so that they sum up to one.

These two steps are repeated for each time step, allowing the filter to adapt to changes in the system over time. The particle filter is particularly effective in situations where the system is nonlinear or the observations are subject to non-Gaussian noise.

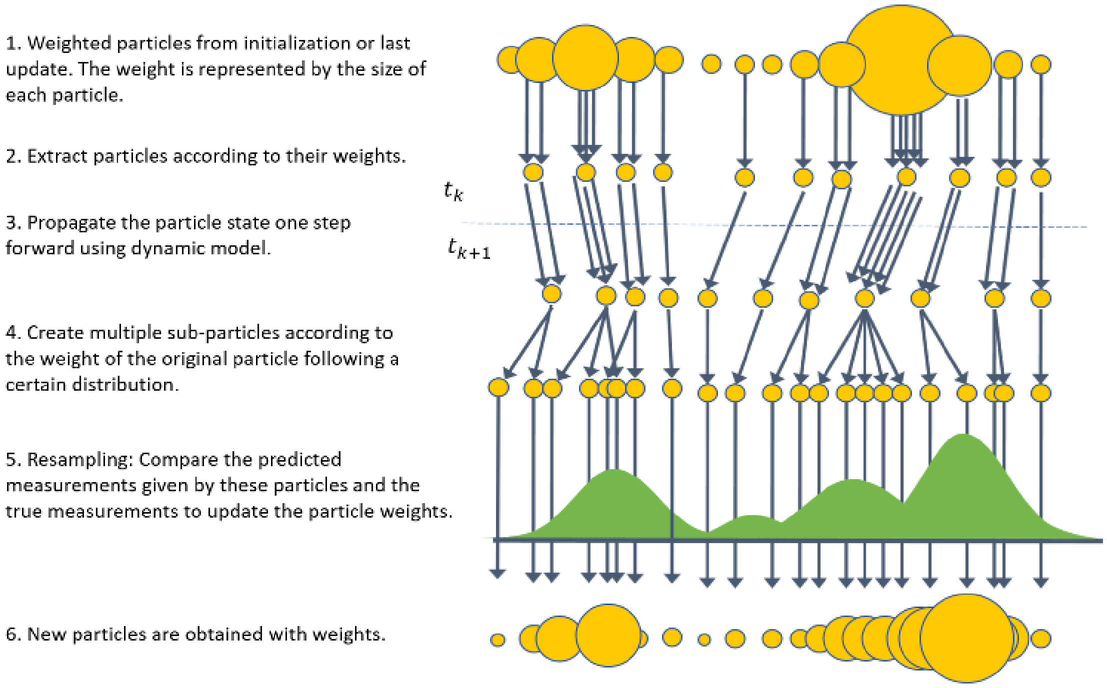

FIGURE 2.9: Enter Caption[43]

2.6 Challenges in Indoor Localization

In this section, we will look at the key challenges encountered in indoor localization. We will discuss each challenge in detail, providing examples and explaining how they affect the performance of indoor localization systems. Understanding these challenges is crucial for the development of effective and robust indoor localization solutions.

2.6.1 Multi-path

Multi-path propagation is a significant challenge in indoor localization systems. It refers to the phenomenon where radio signals, instead of taking a direct path from the transmitter to the receiver, bounce off various surfaces and take multiple paths. This results in the receiver receiving multiple signals from the same source but with different phases and amplitudes [44].

2.6.1.1 Effects of Multi-path

Multi-path propagation can have several effects on the received signal:

- Signal Fading: As the signal takes multiple paths, some paths may be longer than others. This can cause the signals to arrive at the receiver at different times, leading

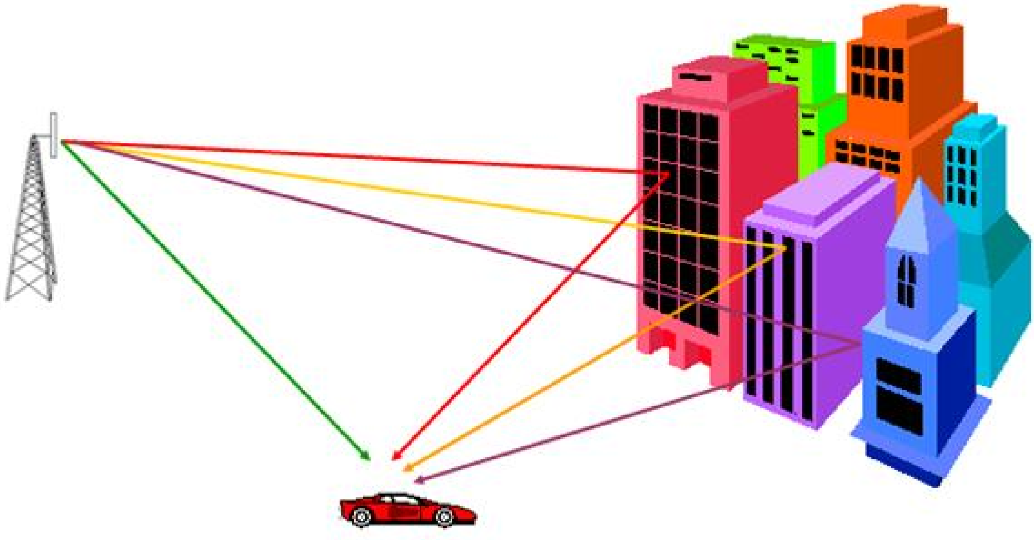

FIGURE 2.10: Multipath propagation (a direct path and several reflections). [45]

to constructive and destructive interference. This interference can cause the signal strength to vary, a phenomenon known as fading.

- InterSymbol Interference (ISI): In digital communication systems, the transmitted signal is divided into several symbols. Due to multipath propagation, symbols can overlap at the receiver, causing Inter-Symbol Interference (ISI). This can significantly degrade the performance of the communication system.
- Time Dispersion: Due to the different path lengths, the signal can spread out over time. This time dispersion can cause the signal to be smeared out at the receiver, making it difficult to distinguish between different signals.

2.6.2 Signal Attenuation

Signal attenuation, also known as signal loss, is a significant challenge in indoor locations. It refers to the reduction in the power density (attenuation) of an electromagnetic wave as it propagates through space. Signal attenuation is a critical factor in the design and performance of wireless communication systems, including indoor localization systems.

Signal attenuation can occur due to various factors, such as distance, interference, and physical obstructions. The strength of the signal decreases as the distance between the transmitter and the receiver increases. This is known as path loss and is a fundamental aspect of signal attenuation.

Interference from other electronic devices or signals can also cause signal attenuation. This is particularly relevant in indoor environments where numerous electronic devices may be operating simultaneously.

Physical obstructions such as walls, doors, and furniture can also cause signal attenuation. Different materials can absorb, reflect, or refract signals to varying degrees, affecting the signal strength at the receiver. For example, a signal passing through a concrete wall will experience more attenuation compared to a signal passing through a wooden partition [46].

2.6.2.1 Impact on Indoor Localization

Signal attenuation can significantly impact the accuracy and reliability of indoor localization systems. For instance, if a system relies on the received signal strength (RSS) to determine the distance between devices, signal attenuation can lead to inaccurate distance estimations and thus inaccurate localization.

2.6.3 Dynamic Environments

Dynamic environments pose a significant challenge for indoor localization systems. These environments are characterized by changes in the physical layout and the presence of moving objects or people. Such changes can affect the propagation of signals used for localization, leading to inaccuracies in the estimated positions.

2.6.3.1 Impact on Indoor Localization

Dynamic environments can impact indoor localization in several ways. Firstly, changes in the physical layout can affect the propagation of signals. For example, moving a large piece of furniture could create a new obstruction to the signal, leading to changes in signal strength at different locations.

Secondly, moving objects or people can cause fluctuations in the signal characteristics used for localization. For example, a person walking past a WiFi access point could cause a temporary drop in signal strength, which could be misinterpreted by the localization system.

Finally, dynamic environments can also introduce new sources of signal interference. For example, electronic devices such as laptops or mobile phones can emit signals that interfere with the signals used for localization.

2.6.4 Limited Line-of-Sight

Unlike outdoor environments, where there is usually a clear line of sight between the sender and the receiver, indoor environments often have limited or no line of sight due to walls, floors, and other obstacles. Indoor localization systems often face the challenge of limited line-of-sight (LoS) conditions. This is due to the presence of obstacles such as walls, furniture, and people, which can block or reflect signals, leading to multipath propagation [47].

In addition to multipath propagation, nonline-of-sight (NLoS) conditions, where the direct path between the transmitter and receiver is obstructed, can also pose significant challenges. NLoS conditions can lead to increased path loss and delay spread, which can adversely affect the accuracy of indoor localization systems.

Various techniques have been proposed to overcome IPS and the NLoS or LoS effects. These include the use of advanced signal processing techniques, such as adaptive filtering and beamforming, as well as the use of additional sensors and information, such as inertial measurement units (IMUs) and floor plans. However, these techniques often require additional computational resources and may not be feasible in all scenarios.

2.6.5 Interference

Indoor localization systems are often subject to various forms of interference, which can significantly impact their performance and accuracy. These interferences can be broadly categorized into two types: physical and wireless interferences.

2.6.5.1 Physical Interferences

Physical interferences refer to the obstacles and structures within the indoor environment that can obstruct the propagation of signals used for localization. These include walls, doors, furniture, and even people. These physical objects can cause reflection, diffraction, and scattering of signals, leading to multipath propagation.

2.6.5.2 Wireless Interferences

Wireless interferences, on the other hand, are caused by other electronic devices and systems operating in the same frequency band. These devices can cause electromagnetic interference, leading to distortion and loss of signals. This can also result in inaccurate distance measurements and hence inaccurate localization.

Furthermore, the presence of other wireless networks can cause interference in the co-channel and adjacent channels. Cochannel interference occurs when two or more networks operate on the same frequency channel, while adjacent channel interference occurs when two networks operate on overlapping frequency channels. Both types of interference can cause signal degradation and loss, leading to inaccurate localization.

Chapter 3

Related work

In the previous chapter, we explored the primary techniques and technologies used in indoor positioning systems (IPS). This chapter will provide an overview of additional work that has been developed to address the challenges of indoor localization.

3.1 WiFi-Based Systems

3.1.1 RADAR

Bahl and Padmanabhan introduced RADAR [48], a pioneering system utilizing RSSI values from user devices to estimate user location. In the offline phase, Access Points (APs) collect RSSI values from user devices to construct a radio map. During the on-line phase, these RSSI values are compared with the offline data to infer user location. RADAR achieves a median localization accuracy of 2.94 meters. The work done in [49] improves localization accuracy by applying a Kalman filter to a system that uses RSSI from WiFi APs. They utilize RSSI fingerprinting in the offline phase to inform position estimation during the online phase. Comparison with a moving average-based system highlights the superior accuracy achieved by the Kalman filter, with a median accuracy of 2.5 meters.

3.1.2 Chronos

Asisht et al. present Chronos [50], a novel MBL system based on a single WiFi Access Point (AP). Chronos leverages Time of Flight (ToF) for precise localization. The AP captures specific beacon messages from the user device and uses them to compute ToF. Achieving precision in localization requires precise ToF estimation down to the order of nanoseconds. To address this, Chronos ingeniously exploits the inverse relationship between bandwidth and time, effectively simulating a wideband system. Both the transmitter and receiver dynamically switch between various WiFi frequency bands, yielding diverse channel measurements. These measurements were amalgamated to derive a reliable ToF estimate.

Once accurately calculated at the AP, these ToF values are translated into distances between each pair of antennas on the AP and the user device. Consequently, both the AP and the client must support Multiple Input Multiple Output (MIMO) functionality. The computed distances are then utilized to derive the 2D locations relative to the AP through an error minimization process, where the deviation between measured and expected distances is minimized. This process adheres to geometric constraints dictated by the antennas' positions on each device.

Despite achieving an impressive median accuracy of 0.65 meters, Chronos exhibits limitations. It lacks scalability and consumes substantial energy as it traverses different frequencies for data collection.

3.1.3 SpotFi

Kotaru et al. introduce SpotFi [51], a groundbreaking localization system that utilizes Channel State Information (CSI) and the Received Signal Strength Indicator (RSSI) to accurately estimate the angle of arrival (AoA) and the time of flight (ToF). These estimates are pivotal for determining the location of the user. Interestingly, SpotFi achieves a remarkable median localization accuracy of 40 centimeters, utilizing standard WiFi cards without requiring any costly hardware components or fingerprinting processes.

SpotFi's methodology involves analyzing signals transmitted from the user device to the Access Point (AP), extracting precise AoA estimates using a limited number of antennas on the AP. In particular, SpotFi observes that multipath effects influence not only the AoA in various antennas, but also CSI in different WiFi subcarriers, due to the variable ToF. To address this challenge, SpotFi employs joint AoA and ToF estimation algorithms, effectively utilizing CSI information.

Although SpotFi demonstrates high accuracy with WiFi APs, it faces limitations in real-time Mobile Localization (MBL) scenarios due to its inability to calculate position estimates with a limited number of signals.

3.1.4 ArrayTrack

Xiong and Jamieson propose ArrayTrack [52], a sophisticated localization system based on precise Angle of Arrival (AoA) calculations at the WiFi Access Point (AP) to estimate user positions. Although ArrayTrack requires a relatively larger number of antennas compared to SpotFi, it achieves a significantly improved median localization accuracy of 23 centimeters.

ArrayTrack operates by detecting packets from various mobile user devices in the AP, requiring only a small number of frames for analysis. Specifically, it samples 10 frames, equivalent to 250 nanoseconds of packet samples in the time domain. Currently, ArrayTrack utilizes short training symbols from the WiFi preamble for packet detection. The system synthesizes independent AoA data from antenna pairs, employing a modified version of the Multiple Signal Classification (MUSIC) algorithm proposed in [53]. To counteract the inherent distortion in AoA spectra, ArrayTrack integrates spatial smoothing techniques by averaging incoming signals across different antennas on the AP.

To mitigate multipath effects, ArrayTrack capitalizes on the relatively stable behavior of the direct Line-of-Sight (LOS) component across different collected samples, in contrast to the variability observed in false peaks or multipath signals. The resulting AoA spectrum is then leveraged to estimate user/device locations.

ArrayTrack boasts high localization accuracy in real-time and scalability. However, its reliance on a larger number of antennas poses a fundamental limitation. Furthermore, its compatibility with standard commercial WiFi APs remains unverified.

3.1.5 Phaser

Phaser [54] builds on the foundation of ArrayTrack, offering indoor localization capabilities using standard WiFi hardware. Employing two Intel 5300 802.11 Network Interface Cards (NICs), each equipped with three antennas, Phaser effectively utilizes a total of 5 antennas by sharing one antenna between the two NICs. This synchronization between the NICs ensures efficient operation. Although Phaser achieves a median accuracy of 1-2 meters, it falls short of the submeter precision often required for indoor localization tasks.

3.1.6 ToneTrack

In contrast, ToneTrack [55] leverages Time of Flight (ToF) data to provide real-time user location estimates with a remarkable median accuracy of 0.9 meters. By combining ToF data acquired through channel or frequency hopping of the user device, ToneTrack employs a channel combination algorithm to enhance time resolution, crucial for precise indoor localization. To address multipath effects and Line-of-Sight (LoS) path absence, ToneTrack employs an innovative spectrum identification algorithm, discerning valuable localization information within the spectrum. Additionally, it utilizes the triangle inequality principle to discard measurements from WiFi APs lacking an LoS path to the user device. Numerical evaluations demonstrate the capability of ToneTrack to provide accurate real-time measurements.

Both Chronos [50] and ToneTrack [55] share the foundational principle of combining information from different channels to improve the accuracy of the localization. However, while ToneTrack has been evaluated with proprietary hardware, its compatibility with existing off-the-shelf WiFi cards remains to be confirmed.

3.1.7 learning-based CSI

In another vein, Wang et al. [56] introduce a deep learning-based indoor Channel State Information (CSI) fingerprinting system. Through an offline training phase, a deep neural network is trained, and in the online phase, a probabilistic method is employed to estimate the user's location, achieving an impressive average localization error of as low as 0.9 meters.

3.1.8 Pallas

Lastly, Luo et al. [57] present Pallas, a system based on the passive collection of received signal strength indicators (RSSI) values in WiFi APs for user localization. Pallas thrives on the passive construction of a WiFi database, initially identifying landmarks within the WiFi RSS traces. By combining this information with indoor floor plans and WiFi AP locations, Pallas maps collected RSS values to indoor pathways, facilitating accurate user localization.

3.2 UWB-Based Systems

3.2.1 Ubisense

Ubisense stands out as a prominent player in the realm of Ultra-Wideband (UWB) based Mobile Localization (MBL) systems, renowned for its impressive accuracy of up to 15 centimeters. Its widespread adoption in industries and commercial sectors underscores its reliability as a solution. However, the substantial cost associated with Ubisense remains a significant hurdle for widespread implementation.

3.2.2 Non-Named Systems

Krishnan et al. [58] introduce a UWB-infrared-based system tailored for robotic applications, extendable to various entities. The system deploys strategically placed UWB readers at known locations, while the UWB transmitter affixed to the robot emits UWB pulses, which are subsequently detected by the readers. Time Difference of Arrival (TDoA) techniques are leveraged to derive an estimate of the robot's location, achieving precise tracking with a Root Mean Square (RMS) error of 15 centimeters.

Shen and Molisch [59] use UWB technology for MBL of various objects, emphasizing the time synchronization between receivers and transmitters to rely on Time of Flight (ToF) rather than TDoA. The authors introduce a Two-Step, Expectation Maximization (TSEM) algorithm, optimizing localization accuracy to attain the Cramer-Rao lower bound for ToF algorithms. Through simulations, the efficacy of this approach is validated, showcasing an error variance approximately 30 decibels lower than existing TDoA-based methods.

Xu et al. [60] utilize TDoA and UWB to locate various blind nodes or users within indoor environments. Accounting for both line-of-sight (LoS) and nonline-of-sight (NLoS) measurements, the authors employ a TDoA error minimizing algorithm to estimate user locations relative to fixed Reference Nodes (RNs), offering a comprehensive solution for indoor localization challenges.

3.3 Acoustics Based Systems

3.3.1 Beep

Mandal et al. introduce Beep [61], a cutting-edge 3D Mobile Location (MBL) system based on acoustic signals. In this setup, diverse acoustic sensors are strategically placed within an indoor environment. These sensors are seamlessly integrated into a central server via a WiFi network. When a user device seeks position services, it sends a request that initiates synchronization with the sensors through the WiFi network. Subsequently, the device emits a predefined acoustic signal, which the sensors utilize to calculate the time of flight (ToF) and convert it into distance measurements.

The distances obtained from all sensor nodes are then relayed to a central server. Here, a sophisticated 3D multi-lateration algorithm is applied to derive an accurate estimate of the user's location. This information is subsequently transmitted back to the user via the WiFi network. Remarkably, the proposed system achieves an impressive accuracy of approximately 0.9 meters in 95% of the experiments carried out.

Although Beep demonstrates remarkable accuracy and apparent scalability, its energy efficiency and latency characteristics warrant a thorough evaluation to determine its practical viability and performance in real-world scenarios.

3.3.2 BeepBeep

Peng et al. propose BeepBeep [62], an innovative acoustic signal-based ranging system designed primarily for proximity detection rather than continuous tracking. What sets BeepBeep apart is its dependence solely on software, eliminating the need for proprietary hardware. Instead, it enables two readily available off-the-shelf devices to perform range analysis and estimate their proximity.

In operation, both devices emit distinctive signals known as "beeps" while simultaneously capturing sounds via their microphones. These recordings encompass the acoustic signals from both devices. By counting the number of samples between the beep signals and exchanging time duration information, BeepBeep computes the two-way Time of Flight (ToF). This approach yields highly accurate ToF measurements, which facilitates a reliable estimate of proximity between the two devices.

Although BeepBeep offers promising proximity estimation capabilities, its reception range may pose challenges in larger spaces. Additionally, its potential for localization applications remains unexplored, leaving room for further investigation and development in this regard.

3.4 RFID Based Systems

3.4.1 LANDMARC

Ni et al. introduce LANDMARC [63], a system that uses active RFIDs for tracking the location of users within indoor environments. In this setup, various RFID tags serve as Reference Nodes (RNs), strategically placed throughout the space. The object to be tracked, such as a user device, is equipped with a tracking tag, while the RNs measure the signals emitted by this tracking tag. In addition, RNs are equipped with IEEE 802.11b cards (Wi-Fi) to facilitate communication with an MBL server. By assessing the strength of the signal from the tracking device, the RNs estimate its location.

Although LANDMARC boasts energy efficiency and an extended range, it does exhibit higher tracking latency and a median accuracy of 1 meter. Moreover, its computational efficiency is lacking, necessitating a higher deployment density for improved localization performance. To address these issues, Jin et al. propose a refined indoor localization mechanism [108]. Rather than relying on measurements between all reference tags and the tracking tag, the authors selectively choose a subset of reference tags based on specific signal strength thresholds. This targeted approach reduces complexity and enhances the accuracy of localization.

3.4.2 RF-Compass

Wang et al. introduce RF-Compass [64], a system that uses RFID on a robot to track various objects equipped with RFID. This innovative approach relies on a novel space partition optimization algorithm to locate the target object. The number of RFID tags on the robot corresponds to the number of space partitions, leading to a tighter localization by confining the target to smaller regions. This increase in RFID tags not only enhances the accuracy of location, but also aids in determining the orientation of the device. RF-Compass achieves an impressive median localization accuracy of 2.76 centimeters.

3.4.3 PinIt

Furthermore, Wang et al. propose PinIt [65], which utilizes the Multipath Profile of RFID tags for localization. PinIt operates effectively even in scenarios where line-of-sight (LoS) is obstructed or in the presence of multipath interference. Reference RFID tags serve as Reference Nodes (RNs), while the multipath profile is constructed by simulating an antenna array through controlled antenna motion. PinIt functions similar to a proximity detection system, querying the desired RFID tag (attached to the target object) and its surrounding tags to pinpoint its location. Despite achieving a median accuracy of 11 centimeters, PinIt faces deployment challenges due to the limited presence of RFID tags on most user devices. Furthermore, its applicability is restricted to specific use cases and cannot be utilized in conventional Mobile-Based Localization (MBL) systems.

3.5 Bluetooth Based Systems

3.5.1 Bluetooth Location Network

Gonzalez-Castano and Garca-Reinoso [66] introduce a Bluetooth Location Network (BLN) for indoor localization, using Bluetooth Reference Nodes (RN) to track user locations. In this setup, Bluetooth-enabled user devices communicate with these RNs, which subsequently relay the user's location information to a master node. This master node is, in turn, linked to service servers.

Inspired by traditional cellular networks, the BLN system achieves room-level accuracy, making it well suited for proximity-based services. However, its response time of approximately 11 seconds renders it non-real-time, limiting its suitability for applications requiring instantaneous location updates.

3.5.2 BIPS

Bruno and Delmastro[67] introduce the Bluetooth Indoor Positioning System (BIPS), a localization solution built on Bluetooth technology. Designed for indoor environments, the BIPS has a short range of less than 10 meters and is known for its energy efficiency. In operation, a Bluetooth enabled user device interacts with fixed Bluetooth Reference Nodes (RNs), which then relay user location estimates to a central BIPS server. Crucially, all RNs are interconnected via a network, facilitating seamless communication and data exchange.

The key functions of the RNs include: a) serving as master nodes to detect nearby slave devices (user devices) and b) facilitating data transfer between users and the RNs. BIPS excels in determining the positions of stationary or slow-moving users within indoor spaces.

Although the authors acknowledge latency and delay concerns, the study lacks explicit commentary on localization accuracy. Notably, the latency of the BIPS system renders it unsuitable for real-time tracking applications, emphasizing its limitations in scenarios requiring immediate location updates.

3.5.3 Bluepass

Diaz et al. introduce Bluepass [68], an innovative Bluetooth-based indoor Mobile Localization (MBL) system that leverages Received Signal Strength Indicator (RSSI) values from user devices to calculate distances relative to fixed distributed Bluetooth receivers. Bluepass comprises several components, including a central server, a local server, a Bluetooth detection device, and a dedicated user device application.

To use the Bluepass MBL system, users must install the application on their devices and log in. The local server is designed to support a single map, while the central server is intended to facilitate the linkage of different maps.

One of Bluepass's notable achievements is its ability to achieve a mean square error (MSE) as low as 2.33 meters, indicative of its impressive localization accuracy within indoor environments.

3.5.4 Zafari

Zafari [[69] uses iBeacons for indoor localization services, collecting received signal strength indicator (RSSI) values from various iBeacons on a user device. These values are then transmitted to a server that runs various localization algorithms. On the server side, Particle Filter (PF), as well as novel cascaded approaches combining Kalman Filter-Particle Filter (KF-PF) and Particle Filter-Extended Kalman Filter (PF-EKF), are employed to enhance localization accuracy. The experimental findings indicate that, on average, PF, KF-PF, and PF-EKF achieve accuracies of 1.441 meters, 1.03 meters, and 0.95 meters, respectively. Although the system boasts energy efficiency and accuracy, it suffers from notable delays and necessitates the deployment of iBeacons, incurring additional costs.

3.5.5 Bluetooth CSI

Ayyalasomayajula et al. [70] introduce a CSI-based localization system utilizing Bluetooth Low Energy (BLE) technology, marking the first instance of such integration to the best of our knowledge. Given the challenges inherent in using Channel State Information (CSI) with BLE, the authors devise BLE-compatible algorithms to overcome various obstacles. Impressively, this approach achieves an accuracy as precise as 86 centimeters.

Islam et al. [71] propose a novel multipath profiling algorithm to track any BLE tag within indoor environments. This technique yields a range error of approximately 2.4 meters.

3.6 Ultrasound Based System

Ashokaraj et al. [72] introduce a deterministic approach named interval analysis [73] that utilizes embedded ultrasonic sensors in a robot for location and navigation within a 2-dimensional (2D) environment. Unlike conventional methods such as Kalman Filters (KF) or Extended Kalman Filters (EKF) [74–76], which often entail a complex data association step requiring linearization, this novel approach bypasses such complexities.

The proposed method assumes the availability of a preexisting map and operates without necessitating any data association or linearization. Although the authors present simulation-based results, the paper does not provide insight into the localization accuracy, latency, or scalability of the proposed technique. It is important to note that the effectiveness of this approach hinges upon the robot's movement and the accurate prediction or estimation of its velocity.

3.6.1 BAT

The BAT Indoor Mobile-Based Localization (MBL) system, as proposed in [77] and evaluated experimentally in [78], utilizes ultrasonic signals for indoor localization. The relatively slower speed of sound waves in air (approximately 330 m/s) offers a notable advantage, significantly improving the accuracy of the localization system compared to other technologies.

In the BAT system, the devices earmarked for tracking are equipped with proprietary transmitters. Fixed and known receivers capture the transmitted signals, utilizing them to estimate the user's location. However, synchronization between transmitters and receivers is imperative for BAT's operation.

BAT achieves an impressive accuracy of up to 3 centimeters in a 3D space [79]. However, its reliance on ultrasound makes it highly sensitive to sensor placement. In addition, the system requires a considerable number of dedicated anchor nodes, which incurs significant costs.

3.6.2 Cricket

The Cricket indoor localization system, as described in [80], employs a fusion of RF and ultrasonic signals for precise indoor positioning. It complements the Bat system by using radio signals solely for receiver synchronization, eliminating the need for transmitter-receiver synchronization.

Unlike Bat, Cricket does not require synchronization between receivers and transmitters. It achieves a commendable accuracy of 10 centimeters [30]. However, its reliance on dedicated hardware and the use of ultrasonic technology restrict its range.

It is pertinent to note that while modern Mobile-Based Localization (MBL) systems predominantly leverage ubiquitous technologies like WiFi, BLE, and visible light due to their widespread availability, the adoption of ultrasound-based systems remains limited. This limitation arises from the lack of ability in most user devices to produce ultrasonic signals. Consequently, the prevalence of ultrasound-based MBL systems is relatively lower.

3.7 Visible Light Systems

Di Lascio et al. introduce LocaLight [81], a novel localization system that uses visible light for Mobile Based Localization (MBL). In LocaLight, RFID sensors strategically positioned on the floor detect variations in light intensity caused by the user's shadow. Equipped with photodiodes, these RFID sensors operate without the need for batteries or external power sources.

In specific configurations, such as optimal LED height, light zone radius, and user height, LocaLight achieves an impressive accuracy of 50 centimeters. However, due to the energy harvesting requirements of RFID sensors, real-time operation is not feasible. Additionally, while effective for proximity detection, LocaLight lacks user-specific information, limiting its suitability for comprehensive MBL applications.

Visible light-based localization systems like LocaLight offer an attractive prospect. However, practical challenges such as energy constraints and hardware limitations make it unlikely that user devices transmit visible light signals for MBL purposes.

Chapter 4

Collection and Data Exploration

To begin exploring the realm of indoor positioning systems, an initial preparation phase was required. This section discusses the use of an online dataset to build foundational knowledge and highlights the emerging need to create custom datasets to further pursue the objectives of this research.

4.1 Initial insights

The study, published in the IEEE Internet of Things Journal[82], carried out several measurement campaigns in various environments, including indoor and outdoor settings.

Concentrating on data from indoor scenarios, the dataset includes times q1,q1,q3, and q4 for all bursts, in addition to their average and an RTT measurement processed by the ESP32. Using this data set, we could explore some initial thoughts to improve accuracy.

Figure 4.1 illustrates a comparison between the Round-Trip Time (RTT) output generated by the ESP32 firmware and the actual RTT measurements (referred to as the 'ground truth'). The scatter plot reveals two distinct trends, represented by two lines.

The first trend line indicates the ESP32's performance at shorter distances, while the second trend line becomes noticeable beyond a certain distance threshold. This suggests that the internal algorithm of ESP32 introduces an offset to minimize the error in RTT measurements at longer distances.

Understanding the intricacies of the internal algorithm of ESP32 would provide valuable information to improve the accuracy of IPS. However, this understanding remains elusive as the algorithm is proprietary and is not available to the public.

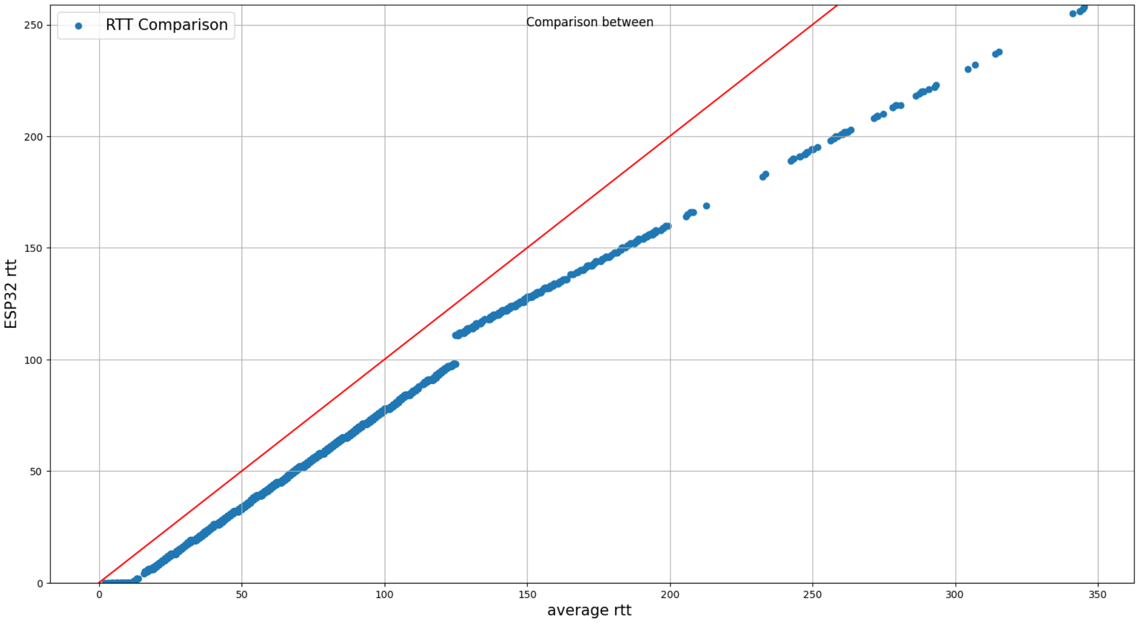

FIGURE 4.1: ESP32 RTT vs Average RTT

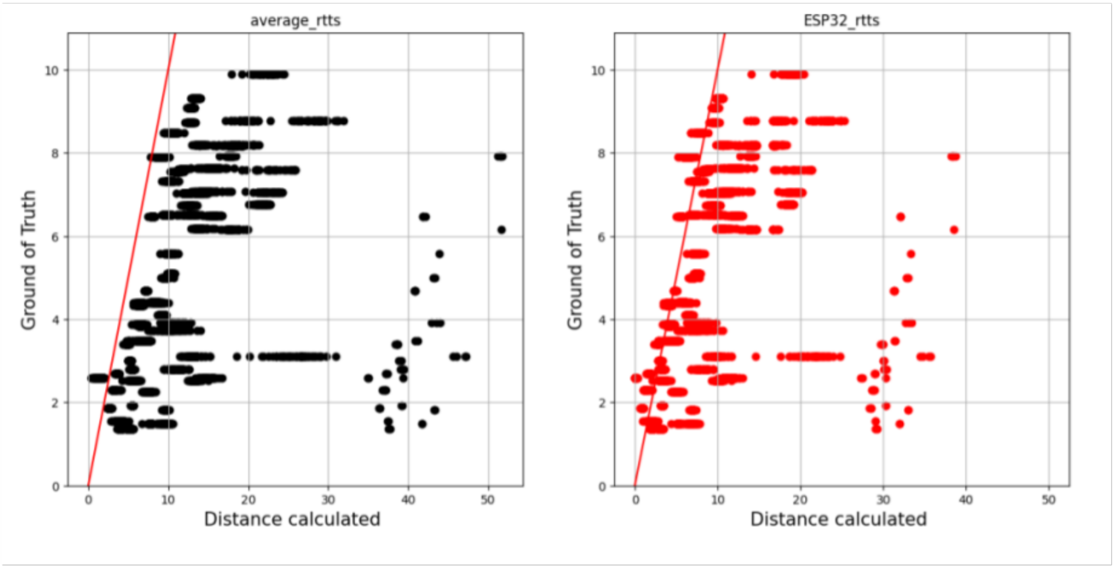

FIGURE 4.2: ESP32 RTT vs Average RTT Distances

Upon examining Figure 4.1, a pivotal query emerges: Between the average and the ESP32-processed RTT, which yields a more precise distance conversion? As Figure 4.2 shows, the distances derived from the ESP32-processed RTT align more accurately with the ground truth. This naturally leads to the contemplation of whether alternatives, such as the minimum RTT or even the first quartile, might provide enhanced precision. Consequently, we embarked on an exploration of various RTT computation methodologies beyond the mere average of each burst. Specifically, we postulated that the briefest time from each burst or the data from the first quartile might offer superior results. To empirically evaluate these theories, we presented side-by-side visual comparisons of each approach compared to the truth of the ground in Figure 4.3, fostering a direct and intuitive assessment. Figure 4.3 presents four distinct plots.

1. The blue plot represents the distance calculated using the first quartile of a burst.
2. The green plot shows the distance derived from the minimum time of a burst.
3. The black plot indicates the distance calculated using the average of the burst.
4. The red plot depicts the distance determined by the RTT processed through the ESP32 algorithm.

Out of these four plots in Figure 4.3, the most accurate representation, aligning closely with the ground truth, is provided by the RTT processed by the ESP32 algorithm.

This analysis for selecting the most accurate processing method may not find direct applications in future contexts of this work. Specifically, the detailed timestamps (q1, q2, q3 and q4) that were pivotal in this analysis are unfortunately not accessible in the Android API 29+ for WiFi RTT, and similarly, in the Decawave DW1001 for UWB technologies. In these platforms, only average time data is available, limiting the depth of analysis we can carry forward into subsequent stages of this research. However, even if not immediately applied, the knowledge gained from this work will be invaluable and on hand for potential future applications or avenues of research.

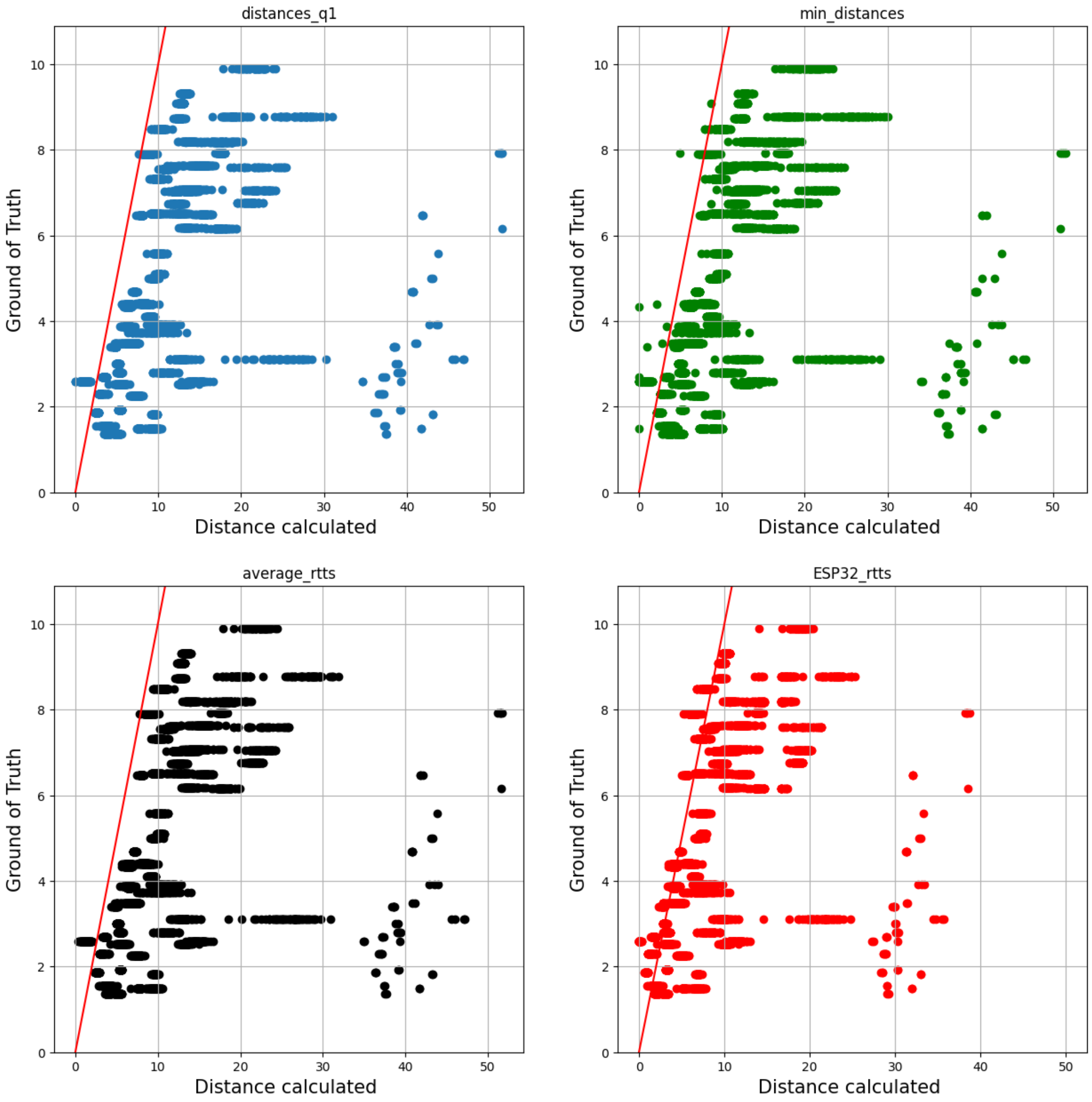

FIGURE 4.3: Comparisons between ground truth, first quartile, minimum points, average, and processed RTT

4.2 Creating Redundancy Rich dataset

Central to our research in indoor localization is the construction of data sets characterized by ample redundancy. Such a comprehensive data set is essential to validate our hypotheses and to understand the intricate dynamics of indoor localization. However, crafting this data set required the development of specialized tools that would be suitable for the task.

Our research blueprint entailed the assembly of four distinct datasets, harnessing the capabilities of two separate technologies – the 802.11mc standard, colloquially known as Wi-Fi Round Trip Time (RTT), and Ultra-Wideband (UWB) technology. Our choice of these technologies was guided by their unique mechanisms and proficiency, which offers a rich array of data for a thorough examination.

Then we created two types of dataset for each technology: static and dynamic. The static dataset, captured with the user remaining stationary, sheds a light on the inherent fluctuations of the FTM measurements in a steady state.

On the other hand, the dynamic dataset was garnered with the user in transit. This data set grants a window into the repercussions of user mobility on FTM readings, elucidating how shifts in mold indoor localization outcomes.

To facilitate the creation of these data-intensive collections, we developed a suite of tools, each specifically designed to enhance the acquisition and organization of FTM metrics. The following sections will provide a more in-depth exploration of these tools, highlighting their crucial contribution to shaping our research direction.

4.2.1 Development of the Android Application for WiFi RTT Data Collection

Initially, we sought online tools or applications that could offer a hands-off approach to collecting WiFi-RTT measurements. However, no suitable online resources were found, highlighting the need to develop our own application.

The Android application was built using Android API-29. It enables requesting Fine Timing Measurement (FTM) data from 802.11mc-capable Access Points (APs). The application allows for pre-configuration of the APs to be used during the data collection phase, as well as on-site selection of APs.

Figure 4.4 illustrates the progression of the interface of the application. The first screen, shown prior to the splash screen, features a ”scan wifi” button. Activating this button transitions the user to the third screen, which displays detected WiFi networks. In scenarios where none of the access points is predefined in the target configuration file, users can simply tap on the MAC address or SSID of a desired access point. This action takes the user to the second screen, providing an interface to dynamically set up and designate the selected access point as a target for FTM requests. The buttons ”Start” and ”Stop” start the FTM requests or stop them.

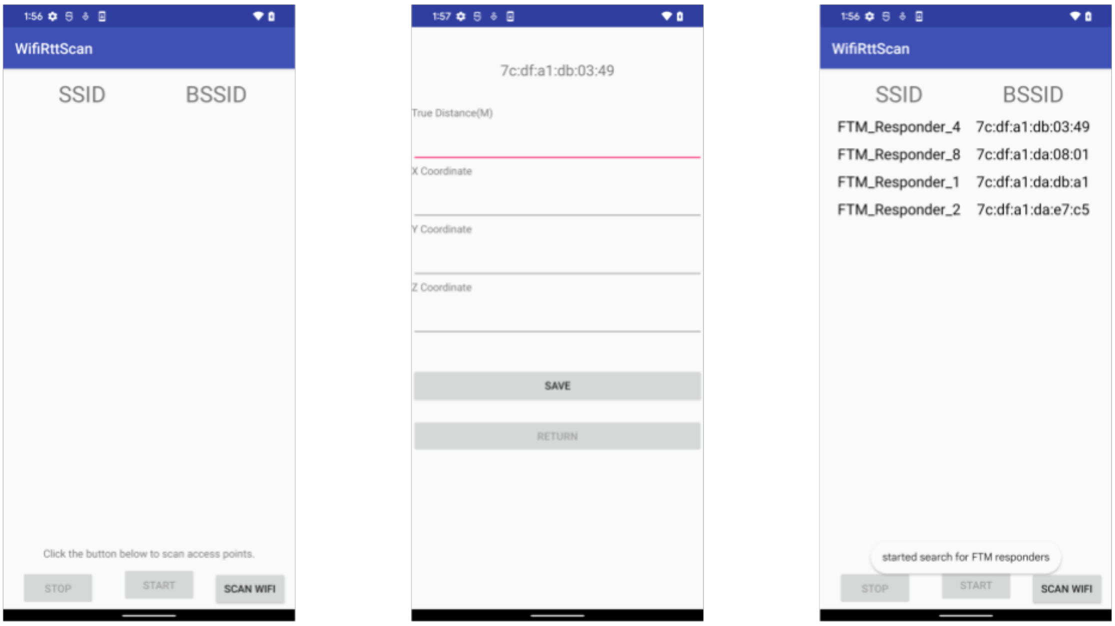

Click the button below to scan access points.

SSID	BSSID
FTM_Responder_4	7c:df:a1:db:03:49
FTM_Responder_8	7c:df:a1:da:08:01
FTM_Responder_1	7c:df:a1:da:db:a1
FTM_Responder_2	7c:df:a1:da:e7:c5

started search for FTM responders

FIGURE 4.4: Android Application for WiFi RTT Data Collection

4.3 Development of Software for UWB Data Collection

Ultra-wideband (UWB) technology, known for its precision in indoor localization, necessitates specialized methods for efficient data collection. Given the versatility and platform-independent nature of Python, we opted for it as our primary tool to develop scripts aimed at collecting data from UWB anchors.

Initially, our focus was on establishing a communication interface with the UWB anchors. Using Python's library ecosystem, particularly 'pyserial', we facilitated serial communication with the anchors. This ensured a consistent and real-time data feed from the devices to our scripts.

To handle potential data flow or interruptions, error handling mechanisms were integrated. This ensured that the scripts remained resilient, logging anomalies while maintaining continuous data capture.

For data storage, a structured approach was employed to maintain consistency with our Android application that collected WiFi RTT data. All captured data was stored in directories labeled as EXP_X, where X denotes the experiment's sequence number. Within these directories, CSV files bearing device ID-based names were placed.

Each CSV file encapsulates a series of records. A record includes a timestamp, the ID of the device, and the acquired measurement. While the timestamp signifies the moment of data capture, the ID provides a reference to the capturing device. The measurement column contains the distance reported.

```
1681211265076,5A0A,6.22
1681211265077,5A0A,5.96
1681211265078,5A0A,6.32
1681211265080,5A0A,6.05
1681211265081,5A0A,6.05
1681211265082,5A0A,6.07
1681211265084,5A0A,5.96
1681211265085,5A0A,5.98
1681211265086,5A0A,6.05
1681211265087,5A0A,6.07
1681211265088,5A0A,6.05
1681211265090,5A0A,6.02
1681211265092,5A0A,6.21
1681211265093,5A0A,6.08
```

(A) Content of a file

(B) Content of a folder

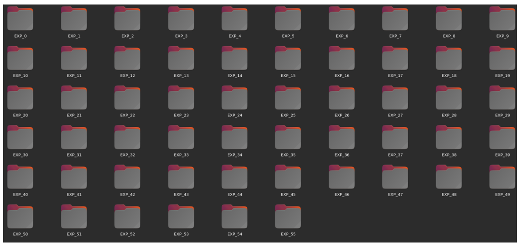

(C) Folder structure

FIGURE 4.5: WiFi RTT tool to data collection process

Figure 4.5 illustrates the structure and content of files and folders. Within a file, each collected measurement displays a timestamp, an anchor ID, and the reported distance. Each folder contains 12 files, with each file corresponding to a unique anchor ID. Moreover, each folder represents a specific collection point.

4.4 Location Data Acquisition and Setup

Selecting an environment for data acquisition is a paramount endeavor. For the research presented in this thesis, our venue of choice was a designated room within the Faculty of Sciences at the University of Porto (FCUP). Traditionally used for experiments related to embedded systems, this room proved to be a great location for our study's specific requirements. Spanning an area of 10m by 6m with a height of 4m, as detailed in 4.6, the room primarily features an expansive open central space. However, desks and chairs strategically placed near the walls introduce elements of both Line-of-Sight (LoS) and NonLine-of-Sight (NLoS) characteristics, essential for a holistic study of indoor localization.

To facilitate precise measurements, the room floor was methodically demarcated into a grid, with each square measuring 1m x 1m, using duct tape. This grid pattern not only

FIGURE 4.6: FCUP Embedded System Room

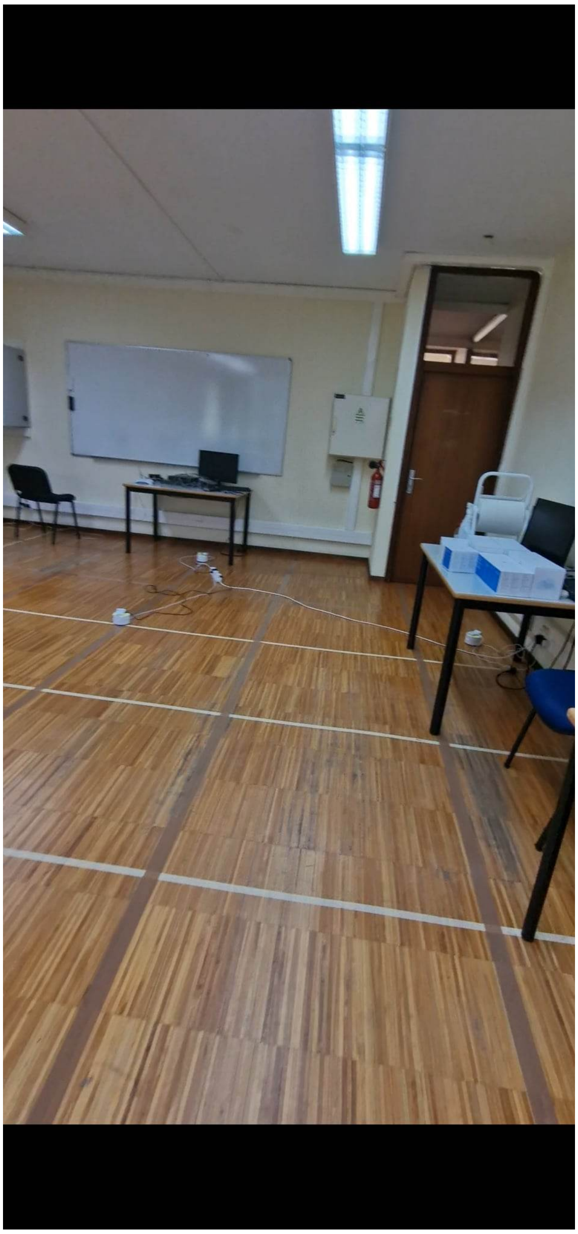

ensured accuracy when placing and measuring both mobile devices and FTM responders, but also served as a clear visual reference for the experimenter.

To further the completeness of our data, 12 distinct points within the room were chosen as the locations of the FTM responders. These placements were diverse, including under desks, next to chairs, and directly on the floor, ensuring a diverse range of scenarios and signal interactions.

In Figure 4.7, the strategic setup of our experimental environment is depicted, where both the 802.11mc Wi-Fi Access Points (AP) and the Ultra Wideband (UWB) tags are located at identical locations within the testing arena, denoted by blue squares. This will

FIGURE 4.7: Environment configuration illustrating the placement of Access Points and UWB tags.

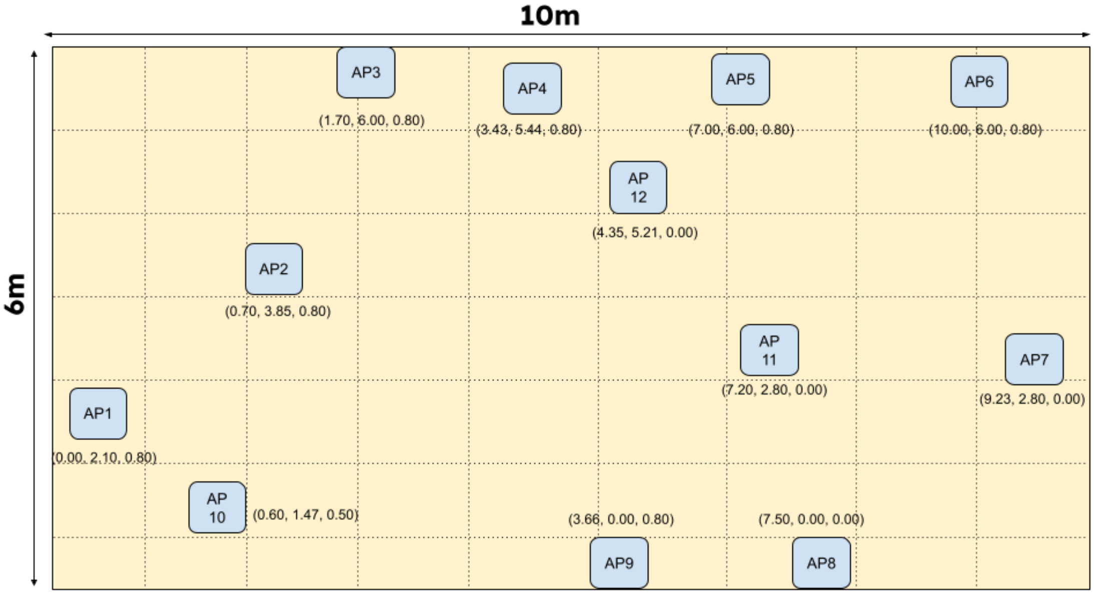

be used to facilitate a direct comparison between the two technologies under identical environmental conditions. The co-location strategy allows for a nuanced analysis of each technology's performance, by eliminating variable factors that could arise from different setups, hence enabling a more accurate and reliable evaluation.

4.4.1 Equipment

The quality and reliability of our data are intrinsically linked to the caliber and functionality of the equipment we use. For our data collection efforts, we rely primarily on three devices: Google Mesh devices, Decawave DWM1001 units, and a Google Pixel 4 smartphone.

The Google Mesh device, known for its reliable propagation of the Wi-Fi signal, is our primary tool for indoor Wi-Fi-based localization. In contrast, the Decawave DWM1001, which emits Ultra-Wideband (UWB) signals, is our preferred device for UWB-based indoor positioning. These devices, each with their unique capabilities, play a crucial role in ensuring the integrity and accuracy of our data collection process.

4.5 Experimentation Methodologies: Static and dynamic

During the static experiment, both the mobile phone and the ultra-wideband tags are strategically placed at the center of each square of the grid. In 10 seconds, data are collected from each square, resulting in a collection of 60 unique datasets. The term ”static” refers to the fixed position of both the mobile phone and the tags throughout the data recording process. This stationary setup allows for a concentrated evaluation of Wi-Fi RTT and ultra-wideband performance, eliminating variables induced by movement.

On the other hand, the dynamic experiment adopts a more flexible approach. The user traces a predetermined path in the room while simultaneously holding the mobile phone and ultra-wideband tags. This continuous data capture, combined with motion, provides a realistic simulation of typical indoor movement. It enables us to delve into the complexities of Wi-Fi RTT and ultra-wideband systems in motion. However, this dynamic framework presents its own challenges. Capturing the true user position with precision requires precision, potentially necessitating the use of advanced tools such as LIDAR. In contrast, static setup, by its very nature, can achieve pinpoint accuracy using simple tools such as a measuring tape, without the need for complex instrumentation.

For the static experiments, the ground truth data were carefully obtained using a meter tape, ensuring precision in every measurement. In contrast, the ground truth for the dynamic experiments was determined based on synchronized waypoints, assuming a consistent speed throughout the path. Although this dynamic method may not provide the exactness of its static counterpart, it was the most practical solution available.

Figure 4.8 illustrates the strategic locations chosen to conduct the static experiments within a designated room. Although not scaled to exact real-world proportions, the figure serves as a visual guide, offering an insightful glimpse into the experimental setup. The room, with dimensions marked 10x6, is delineated in a grid, where each cell has 1 m^2 and represents a specific focus area in the room.

In the center of each grid square, a point is distinctly marked, symbolizing the precise location where the static experiments were executed. These central points, evenly distributed across the grid, ensure a comprehensive analysis covering the entire area of the room.

Figure 4.9 illustrates that the trajectory taken during dynamic experiments is vividly delineated, offering a clear visualization of the movement path and the synchronization

FIGURE 4.8: Static Experiment

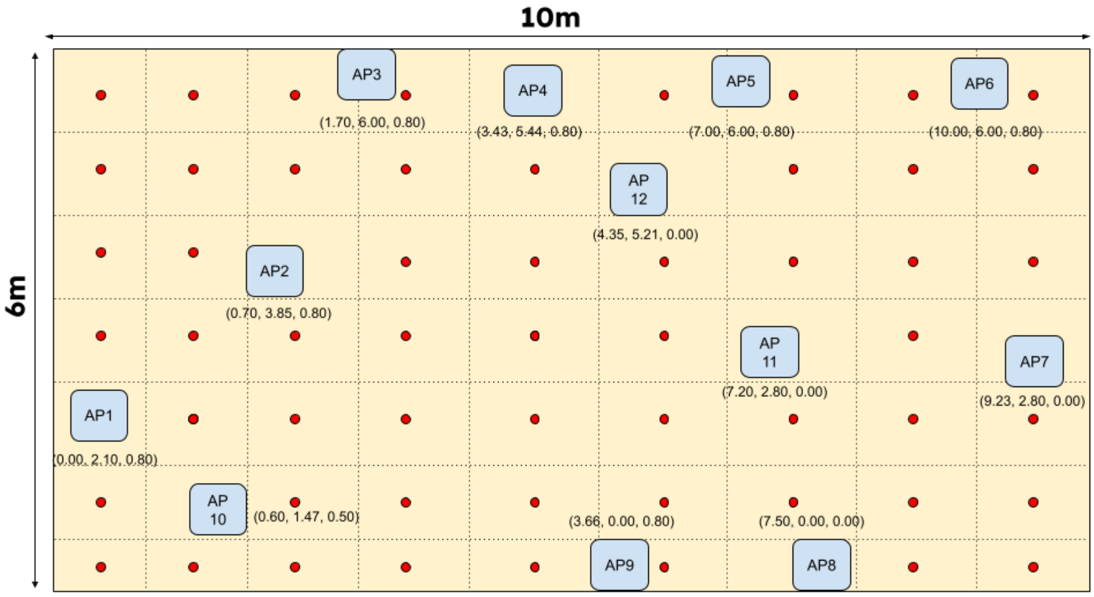

FIGURE 4.9: Dynamic Experiment

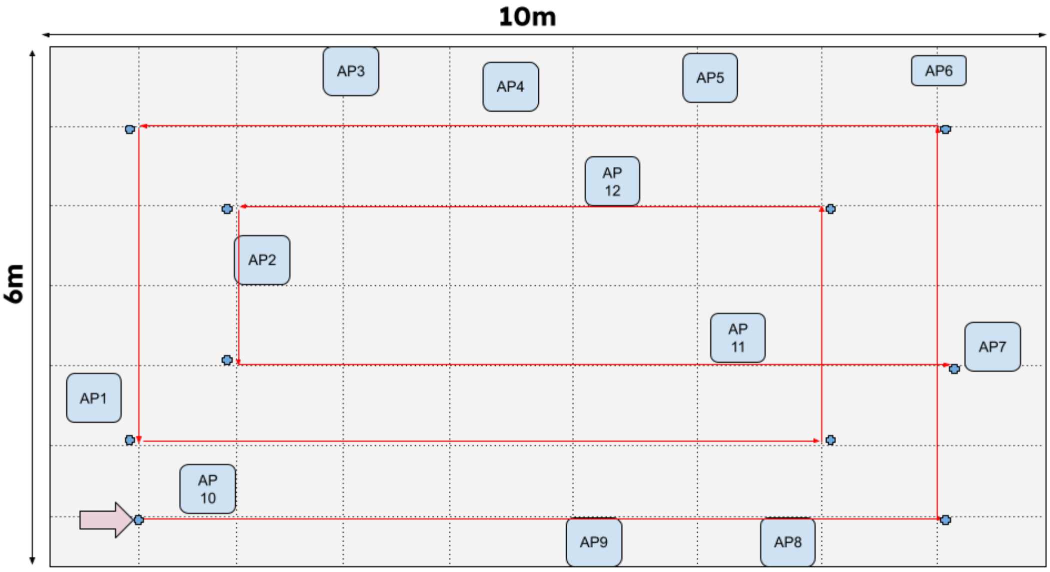

points. The journey begins at the location indicated by a prominent pink arrow, which signals the starting point of the dynamic path.

As we trace the path further, marked by a series of red arrows, it guides us through the intricacies of the movement pattern adopted during the experiment. Furthermore, the figure is punctuated with blue crosses at every corner of the path, where a change in direction occurs. These blue crosses, termed sync points, play a pivotal role in the experiment. They mark the specific junctures where synchronization activities occur.

4.6 Challenges in Experimentation

Throughout indoor localization experiments, various technological intricacies and device-specific limitations presented themselves as formidable challenges.

With the ultra-wideband data collection involving Decawave DWM1001 devices, we grappled with a unique constraint: each tag could simultaneously associate with only four anchors. Given that our set-up incorporated 12 anchors, it necessitated the deployment of three distinct tags, each possessing a different network ID. This layered arrangement added to the experimental complexity. Not only was it crucial to confirm the precise association of each tag with the appropriate anchors, but it was equally crucial to amalgamate the data from the diverse tags seamlessly.

However, the acquisition of 802.11mc data, facilitated by Google Mesh devices, brought its own set of challenges. Securing consistent responses from all 12 access points (AP) proved to be a complex task. However, in spite of these hurdles, the rigorous process yielded a substantial data set, prepared for meticulous analysis in subsequent phases.

Chapter 5

Data Analysis

This chapter analyzes the data acquired in the previous chapter, outlining strategies to understand the relationship between using more than the minimum required measurements for location computation. It also lays the foundation for an innovative solution that leverages FTM redundancy to enhance accuracy.

5.1 Bias Detection through Ground Truth and Calculated Distance Correlation

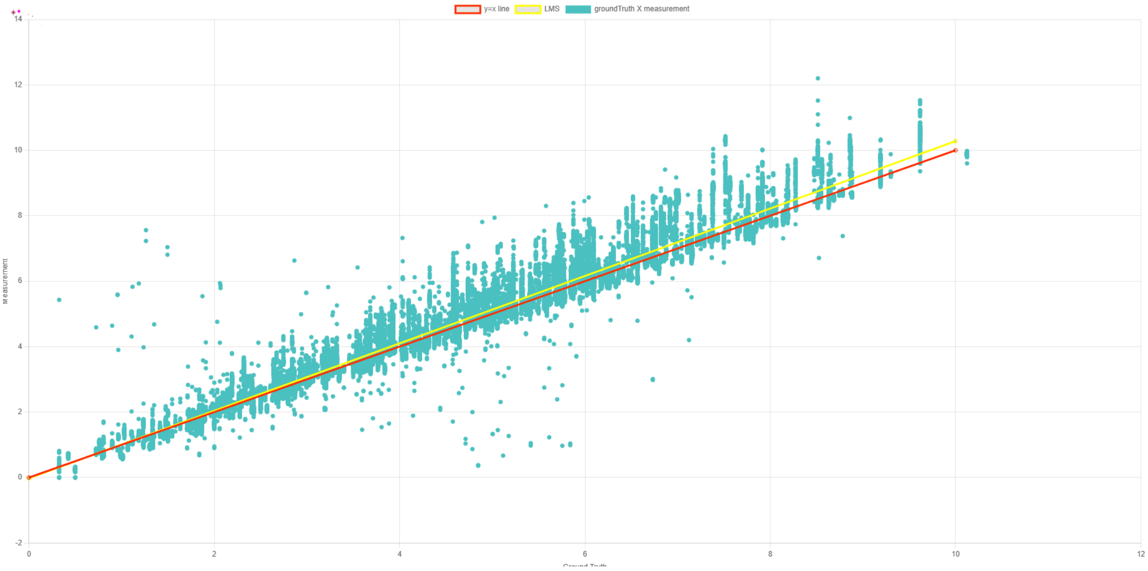

FIGURE 5.1: LMS in UWB Data

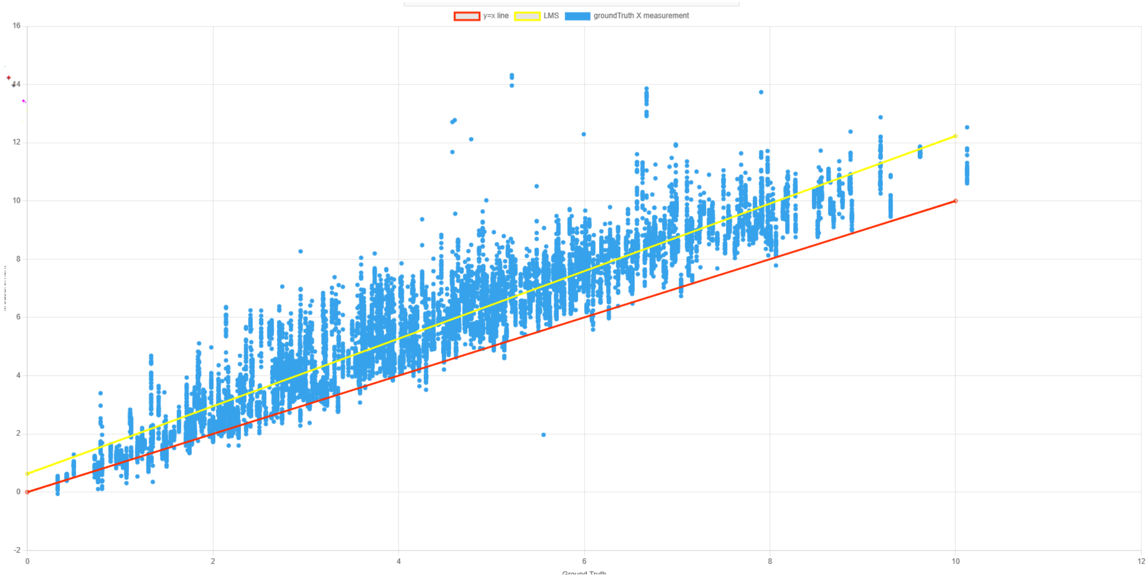

FIGURE 5.2: LMS in Wifi RTT Data

Before delving into data analysis, it is crucial to identify and address the systematic biases inherent in each technology used. These biases, which arise from consistent measurement deviations, can significantly distort data interpretation and conclusions. Such discrepancies may be due to hardware limitations, environmental interferences, or software-related issues.

To address the systematic biases of our data, we turned to the Least Mean Squares (LMS) method. The LMS approach was crucial in pinpointing and quantifying any systematic bias evident in our readings. Our analysis rendered the LMS line for UWB measurements as $y = 1.03x - 0.02$, while for WiFi RTT measurements, it stood at $y = 1.16x + 0.63$. These LMS equations shed light on the inherent biases in each technology, guiding us toward potential corrective interventions.

An ideal scenario, in which the measurements impeccably mirror the truth of the ground, would be represented by a $y = x$ line. By juxtaposing our data points and the LMS line against this ideal line, we discern the degree of alignment and potential biases inherent to our systems. For a more tangible comparison, Figures 5.1 and 5.2 illustrate these relationships for the UWB and 802.11mc measurements, respectively.

Our analytical efforts revealed the superiority of UWB technology in terms of precision. This was evident from the LMS line for UWB, indicating a less biased $y = 1.03x - 0.02$ compared to the 802.11 mc readings $y = 1.16x + 0.63$. This comparative advantage of UWB translates into numerous benefits.

- A reduced bias suggests a closer adherence to the ground truth, hinting at UWB's innate advantage in accurate indoor localization relative to the 802.11 mc system.

- The necessity for corrective adjustments diminishes with a reduced bias. Consequently, the UWB system demands less intensive corrections, streamlining the overall calibration process.

- The lesser the bias, the greater the reliability. The minimized potential for pronounced localization errors renders UWB as the preferred option in applications where precision is pivotal.

5.2 Spatial Reconstruction from Distance Data

A fundamental step in indoor localization is the transformation of distance measurements into actual coordinates within a space. Once the systematic bias inherent in the data of each technology was identified and addressed in our preliminary analysis, we were poised to tackle this transformation with increased accuracy.

The method of choice for this transformation was the Gradient Descent algorithm, a powerful optimization tool widely used in machine learning and computational geometry. Here is a brief overview of the process:

1. **Initialization:** We start by initializing random positions for the devices within the defined space. The aim is to adjust these positions iteratively until the calculated distances closely match the corrected measurements we obtained.

2. **Objective Function:** Our goal was to minimize the difference between the corrected distance measurements and the Euclidean distances calculated from our initial position guesses. The objective function, or cost function, quantifies this difference for each iteration.

3. **Gradient Computation:** At each iteration, the gradient of the objective function with respect to each device's position was computed. This gradient indicates the direction and magnitude of the necessary positional adjustments to minimize the cost function.

4. **Position Update:** The positions of the devices were updated in the direction of the negative gradient, with a learning rate controlling the step size. This iterative process ensures that with each step, the estimated positions better reflect the corrected distance measurements.

5. **Convergence:** The algorithm iteratively refines device positions until the change in the objective function falls below a predefined threshold, or a set number of iterations is reached. The resulting positions represent our best estimate of the devices' locations in the space.

Theoretically, having four distances is sufficient to pinpoint a location in a 3D space, provided that we have a nondegenerate configuration. However, in our experimental setup, we had the advantage of obtaining data from 12 different sources, which is significantly more than the basic requirement. This wealth of distance data opens up an intriguing possibility: the opportunity to evaluate various combinations of distances and observe their impact on the resulting spatial estimates.

By examining all distance combinations, starting from the minimum of 4 and scaling up to the full set of 12, we can identify patterns, redundancies, or even anomalies in how these combinations influence the distribution of points in our 3D space. This comprehensive analysis allows us to gain deeper insight into the spatial dynamics of our system.

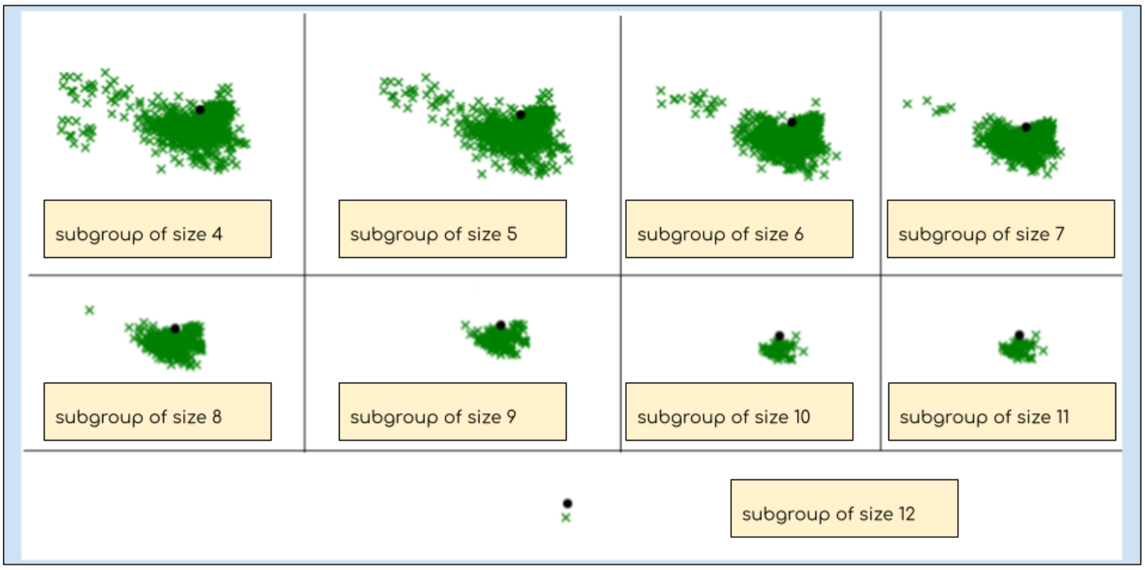

FIGURE 5.3: Constellation Of Points UWB

Analyzing Figures 5.3 and 5.4, a fascinating observation emerged. Although one might instinctively assume that using the full set of distance measurements would yield

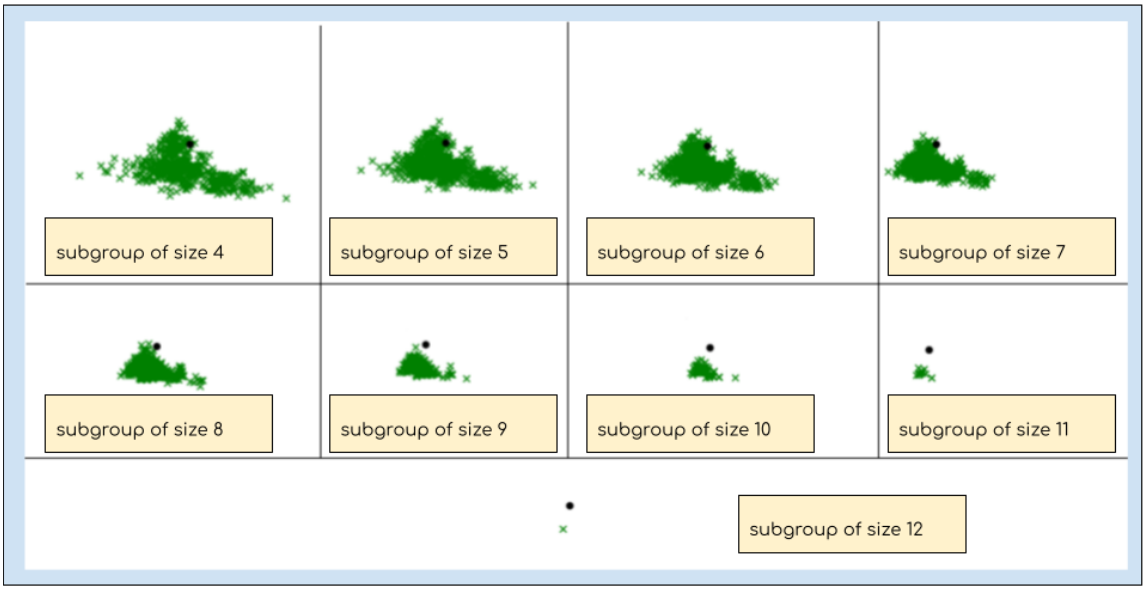

FIGURE 5.4: Constellation Of points WiFi

the most accurate results, our experiments revealed a more nuanced reality. When we considered subgroups of distance measurements that did not encompass the entire set, several combinations astonishingly pinpointed the exact location corresponding to the ground truth. In some instances, in addition to not outputting the same ground truth point, these subsets outperformed the complete set, producing a smaller error in the derived position.

This finding has profound implications for our localization efforts. It suggests that there is an optimal combination of distance measurements — a sweet spot — that can be more effective than simply harnessing every available data point. This not only challenges conventional wisdom, but also presents an opportunity. By intelligently selecting the most impactful subset of measurements, we can potentially enhance the accuracy of our positioning system, making it more efficient and reliable.

After examining the compelling findings of the static scenarios presented in Figures 5.3 and 5.4, a natural inquiry surfaced: Does this trend of attaining enhanced accuracy with measurement subsets pertain solely to static environments, or does it have implications for dynamic scenarios, too?

To investigate this further, we turn our attention to Figures 5.5 and 5.6, which showcase the results of the dynamic experiments. The observed patterns were consistent with our previous findings for the UWB measurements. Remarkably, even under dynamic conditions, certain subsets of measurements still managed to achieve results close to or even surpassing the accuracy derived from using the entire set.

However, the WiFi RTT measurements presented a contrasting story. Despite exploring various combinations, the WiFi RTT performance was noticeably suboptimal across all subsets in the dynamic scenario. This divergence underscores the inherent challenges and limitations of relying solely on WiFi RTT for indoor location, especially in settings marked by movement and variability.

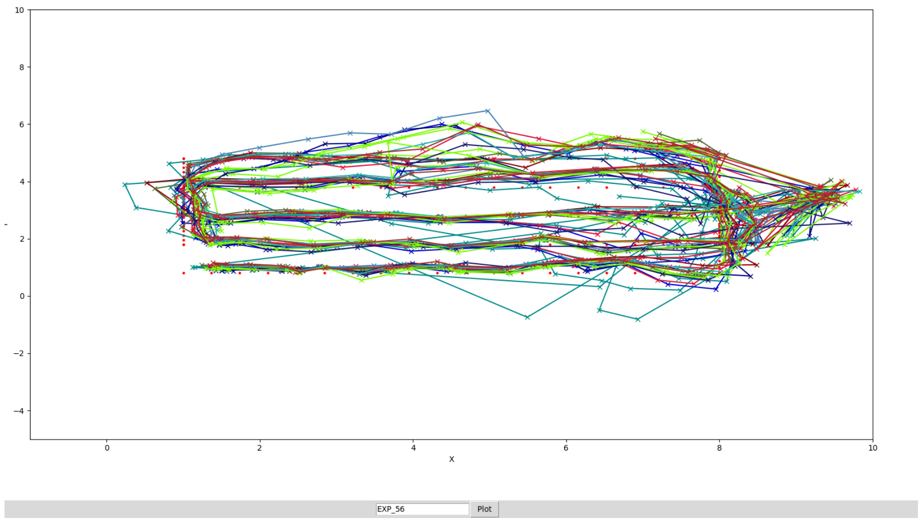

FIGURE 5.5: Path Using UWB Data

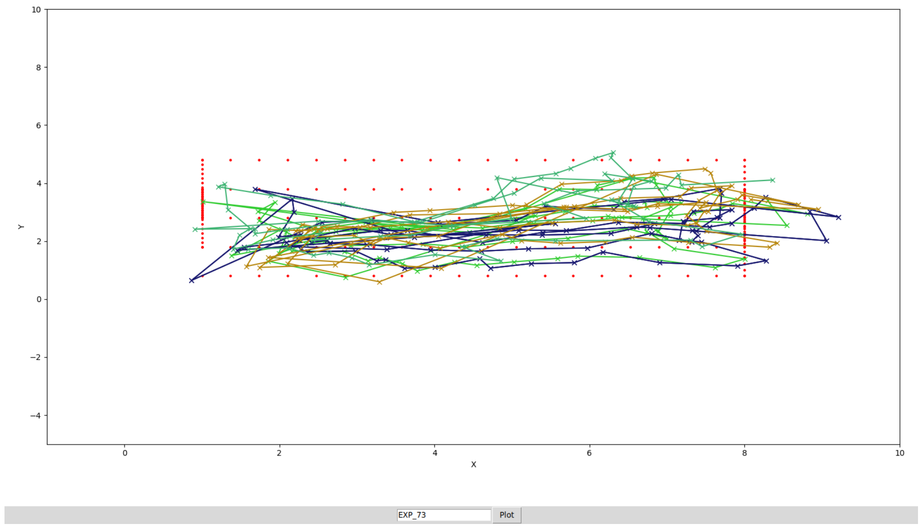

FIGURE 5.6: Path Using WiFi Data

Upon meticulous examination of the plots delineated in Figures 5.3, 5.4, 5.5, and 5.6, we initiated a comprehensive investigation of the potential variations in results when alternating the positions of the Ultra-Wideband tags and WiFi access points. This analytical endeavor sought to discern whether the accuracy and reliability of the localization could be impacted by modifications in the configuration of the setup.

Preliminary analysis indicates a marginal alteration in results when the ultra-widthband tags and WiFi access points were relocated. This suggests a degree of stability and robustness of both technologies regarding the hardware utilized, wherein the positioning of tags and access points does not significantly influence the precision of the localization. However, it is pertinent to perform further analyses to corroborate these initial findings, exploring potential underlying factors that could contribute to the minor discrepancies observed.

5.3 Data Analysis Remarks

The experimental results show that UWB, even without any additional processing steps, achieves high fidelity in both the static and dynamic cases. This underscores the robustness of UWB technology in tracking positions accurately under different conditions.

However, WiFi RTT 802.11 mc, as per our findings, does not seem to provide a satisfactory position estimation when simply converting measurements to locations. This suggests a need for an additional processing step to improve its performance in indoor localization tasks.

However, the presence of extremely close matches to the real location in the constellation of points for both technologies offers a promising avenue for such improvements. By harnessing these close matches and possibly integrating additional data processing or filtering techniques, we could potentially improve the accuracy of WiFi-based indoor localization.

These findings provide a solid foundation for the subsequent chapters of this thesis, where we will dive deeper into potential strategies to improve localization accuracy, particularly for WiFi RTT 802.11 mc.

Chapter 6

Proposed Solution

6.1 Introduction

This thesis presents a novel approach to indoor localization that improves precision by leveraging redundancy in access points (AP) or anchors. The central focus is developing an algorithm capable of reducing the constellation of points derived from multiple APs or anchors into a single precise location estimate.

The proposed method begins by identifying the available Fine-Time Measurement (FTM) responders in the environment. These responders are then divided into subgroups, each representing a subset of the total responders. For each subgroup, a constellation of potential location points is generated on the basis of distance measurements. The crucial point of this approach lies in applying a dedicated algorithm to consolidate these constellations into a single point, which serves as a more accurate estimation of the actual location.

One of the key advantages of this approach is its ability to mitigate common challenges in indoor localization, such as multipath propagation. By focusing on the reduction of point constellations into a singular location estimate, the algorithm effectively filters out inaccuracies and noise that often compromise localization precision.

In the following sections, we will explore the details of this approach, including the methodology for subgroup creation, the specific algorithm designed to consolidate constellations into a single point, and the techniques used to minimize the effects of multipath propagation.

6.2 Distance Measurements to Location

In the initial phase of our proposed methodology, we employ a lateration technique to convert distances into spatial coordinates. Specifically, we utilize the gradient descent algorithm for this purpose.

To accomplish this, we form subgroups of a specified size and transform each subgroup of distance measurements into a single point. This procedure results in a constellation where the total number of points corresponds to the number of subgroups formed.

It is important to highlight that the size of each subgroup is not predetermined for this algorithm. This parameter requires careful adjustment according to the specific configuration of each environment.

6.3 Consolidation of the Constellation

Once the constellation of points has been generated from the subgroups of measurements, the subsequent challenge is to convert these points into a singular position estimate that signifies the location of the user. To address this, we have investigated and experimented with three distinct strategies: a clustering technique, a minimum distance computation, and a secondary implementation of the gradient descent algorithm.

- **Clustering Approach (DBSCAN)**: In this method, we applied the Density-Based Spatial Clustering of Applications with Noise (DBSCAN) algorithm to the constellation of points. DBSCAN is a popular clustering algorithm that groups together points that are packed closely together (points with many nearby neighbors). After identifying the clusters in our constellation, we selected the cluster with the most points and calculated the mean position of these points to represent the estimated user location.

- **Minimum Distance Calculation**: In the second approach, we identified the point in the constellation that had the minimum Euclidean distance to all other points. The rationale behind this method is that this point could potentially represent a central location that minimizes the total distance to all other points in the constellation.

- **Gradient Descent Reapplication**: The third approach involved a secondary application of the gradient descent algorithm. This time, the algorithm was applied to the constellation of points with the aim of minimizing the total Euclidean distance between the calculated position and all the points in the constellation.

A question that might arise is: Why choose DBSCAN as the clustering algorithm instead of another option? The selection of DBSCAN hinges on its inherent advantage: it does not require a predetermined number of clusters. Instead, the number of clusters produced is solely dependent on the dataset and its inherent structure, determined by factors such as density and proximity of data points. This adaptability makes DBSCAN particularly suitable for situations where the true number of clusters is unknown or may vary across different datasets.

Unlike partitioning-based clustering methods, such as K-means, DBSCAN operates on the basis of density connectivity. In this context, a cluster is a densely populated region of data points segregated by less dense areas from other clusters or noise. The DBSCAN algorithm is characterized by two primary parameters:

1. **MinPts**: The minimum number of points required to form a dense region or cluster.
2. **Epsilon (eps)**: The maximum distance between two data points for one to consider them as part of the same cluster.

For our research, we set *MinPts* to 5, as this group size demonstrated optimal performance during analysis in our test environment. Moreover, we have defined an epsilon value of 0.2, indicating that two points must be within 20cm of each other to be categorized within the same cluster.

Using these parameters, DBSCAN explores the data and expands the clusters based on the density of points. This ensures that the clusters are spatially coherent and distinctly separated from other clusters or outliers.

Regarding the min_point method and the gradient descent method, which yielded the best results, both methods share similarities in their aim of minimizing a certain "cost function." The primary distinction lies in their outputs. Although the `min_point` method always selects a point from the given constellation, the gradient descent approach can produce a point that might not necessarily belong to the original constellation.

Up to this point, if the application targets a stationary situation, the algorithm can stop. However, for dynamic situations, a third phase can be introduced.

Figure 6.1 illustrates a comparison among four methods for consolidating a constellation of points into a single point.

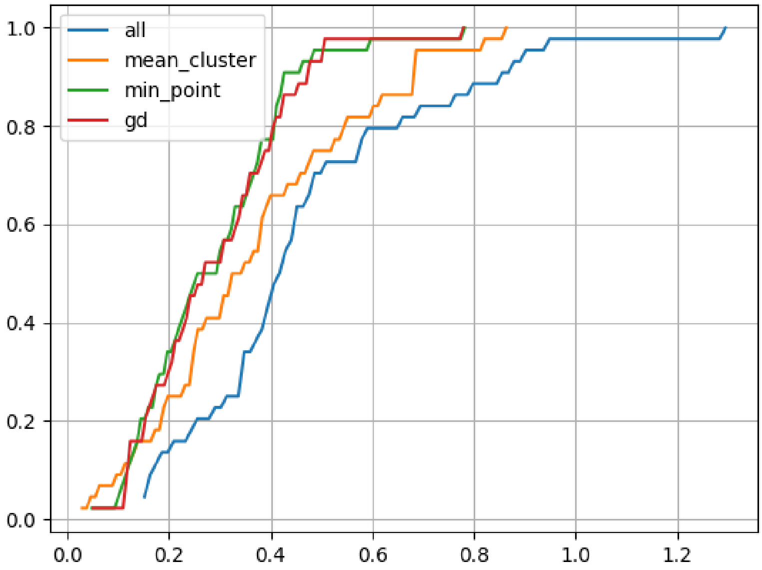

FIGURE 6.1: CDF Step 2 Comparison

- In blue, the single point is derived from the average of all points in the constellation.
- In green, the selected point is the one with the minimum distance to all other points in the constellation.
- In orange, the DBSCAN algorithm identifies a cluster, and the average of this cluster determines the point.
- In brown, the gradient descent method is applied to the constellation of points.

From the results in the chosen environment, both the ”min_point” strategy and the gradient descent (gd) method yield the most favorable results. As observed in Figure 6.1, 80% of the points calculated using these strategies result in errors less than 40 cm.

6.4 Dynamic Situation Tracker

When tracking a device in motion, the use of historical data can markedly improve the precision and consistency of location estimates.

A uniform movement, such as forward progression, will produce points that largely align with each other, preserving an anticipated trajectory. However, complications arise when an outlier appears, for instance, a point indicating a reverse movement that deviates from the expected path.

To address this, the algorithm can be configured to postpone immediate responses to such anomalous data. Instead, it awaits subsequent points, for example, the next three, to confirm this unexpected direction. If all three points agree with the initial outlier, indicating a legitimate reverse movement, the algorithm can adjust the location accordingly. However, if these points contradict the outlier, it can be classified as an anomaly, thereby preventing it from affecting the output.

This strategy ensures that the user experiences a smooth, continuous movement, without the abrupt shifts that might result from sporadic data anomalies.

6.5 Comparison with Existing Solutions

Unfortunately, we were unable to perform a direct comparison with any existing solutions due to time constraints. Moreover, a fair comparison can only be conducted if both the existing solution and our approach are tested in the same environments, which was not feasible within our timeframe.

However, based on our initial evaluations, the solution exhibits promising results. Specifically, 100% of the data produced by our solution falls under a localization error of 0.9m, demonstrating significant potential in terms of accuracy and performance. We anticipate that, with further refinements and testing in various environmental conditions, our solution could potentially supersede existing solutions on the market, offering a more accurate and reliable alternative for localization applications.

6.6 Robustness Analysis

In the development and evaluation of our solution, significant emphasis has been placed on its resilience to noise and disturbances commonly encountered in real-world environments. These disturbances can be manifold, ranging from electromagnetic interference to physical obstacles disrupting the direct line of sight.

The initial testing phases have demonstrated a commendable level of resilience to such disruptions, primarily due to the robust nature of the algorithms deployed in each step of the solution. Specifically, the gradient descent and clustering techniques utilized are known to mitigate the effects of noise, yielding more accurate results even under less ideal conditions.

Furthermore, the time window implemented in Step 3 acts as a filtering mechanism, helping to smooth out the potential noise and anomalies in the data, thus further enhancing the resilience of the system. In future developments, our aim is to integrate more sophisticated noise reduction techniques and predictive algorithms to elevate the noise resilience of the solution to an even higher standard.

However, it is pertinent to note that the resilience of the system can be heavily influenced by the choice of parameters and settings at each step of the algorithm. Hence, a careful and considerate selection of these parameters is vital to maintaining a high level of resilience to noise and disturbances.

6.7 Potential Improvements and Future Directions

As we strive to improve the efficacy and accuracy of our solution, there are several avenues for potential improvements and directions that we intend to explore in future iterations of development. The following points illustrate some of the significant areas where further advances can be achieved.

- **Integration of Additional Data Sources**: To foster a more robust and precise localization performance, the incorporation of data from additional sources such as inertial sensors can be a pivotal step. These sensors can provide auxiliary data points which, when integrated into the existing solution, have the potential to significantly bolster the accuracy and reliability of the localization results.
- **Exploration of Machine Learning Approaches**: The current solution primarily relies on mathematical and statistical approaches for data processing and analysis. However, leveraging machine learning techniques can pave the way for a more intelligent and adaptive system. Through the application of machine learning algorithms, the system can learn and adapt to the nuances of different environments, potentially offering more accurate localization even in dynamically changing conditions.

By focusing on these improvements and constantly adapting to emerging technologies and methodologies, we aspire to develop a solution that not only meets current needs but also remains resilient and adaptable in the face of future challenges and developments.

Chapter 7

Conclusion

The initial stages of this project were marked by an intensive phase of tool creation. The creation of tools that could integrate seamlessly with Wi-Fi RTT and UWB technologies presented a steep learning curve. The effort was not only to develop functional tools but also to create instruments that could capture data with a high degree of accuracy and reliability, thus laying a robust foundation for the subsequent stages of the research.

Furthermore, the development of the datasets was a time-consuming process. Preparing the environment to be conducive for data collection involved a detailed analysis of the space. This phase of the investigation was critical, as the quality of the data sets would significantly influence the outcome of the study.

Adding to the complexity of the investigation were the initial encounters with sophisticated filtering techniques such as the particle filter and the Kalman filter. Understanding and implementing these algorithms proved to be a challenging undertaking.

However, with persistent effort and commitment, the author managed to overcome these challenges. The process of grappling with complex algorithms and creating robust tools not only facilitated the successful completion of this research but also contributed to a significant expansion of the author's skill set and knowledge base.

7.1 Observed Advantages Using WiFi RTT

The use of WiFi round trip time (RTT) reveals several advantages that can contribute to the potential success and efficacy of IPS. Here, we delineate the observed benefits of employing WiFi RTT in our solution:

- **Infrastructure Utilization**: In environments equipped with WiFi infrastructure, the utilization of WiFi RTT can be seen as a cost-effective solution. It leverages existing infrastructure, reducing the need for deploying additional hardware and thereby potentially lowering the implementation costs.
- **Integration Opportunities**: WiFi RTT can be seamlessly integrated with other technologies and data sources, such as inertial sensors and machine learning approaches, to further enhance the solution's capabilities. This integration opens up avenues for further innovation and improvements in localization performance.

7.2 Observed Advantages Using Ultra Wide-Band

In the course of our research and development, we have noted numerous advantages attributed to the utilization of Ultra Wide-Band (UWB) technology. In the following, we enumerate the observed advantages of employing UWB in our solution:

- **High Accuracy and Precision**: UWB technology is renowned for its ability to offer high accuracy and precision in localization tasks. By leveraging the wide bandwidth of UWB signals, our solution can achieve fine resolution and a lower error margin, thus enhancing the reliability of the localization process.
- **Penetration Capability**: UWB signals are capable of penetrating through obstacles such as walls and furniture, which makes it a suitable choice for indoor localization scenarios where line-of-sight is not always guaranteed. This penetration capability ensures a consistent performance even in complex environments.
- **Integration with Other Technologies**: Similar to WiFi RTT, UWB can also be integrated with other technologies and data sources to further refine the solution. The potential integration with inertial sensors and machine learning approaches, for instance, can pave the way for a more versatile and adaptive localization solution.

7.3 Software developed to assist research work

In addition to the primary software tools discussed in the previous chapter, this work also contributed to the development of additional software utilities. Although the initial focus was on software that aimed to capture and analyze data for indoor localization, there was an equally important need to visualize these data effectively. The visualization software complements the analytical tools by offering 2D and 3D perspectives, enriching the interpretation of the indoor localization metrics.

The codebase for these additional tools is freely available on my personal GitHub account under an open source license. All the software is written in Python.

Figures 7.1 and 7.2 display the user interface of the software component. This software enables users to visualize data from any dataset, provided that it is formatted as expected by the software. It also allows users to pinpoint locations in both 2D and 3D, and offers the flexibility to switch between datasets and adjust the group size dynamically.

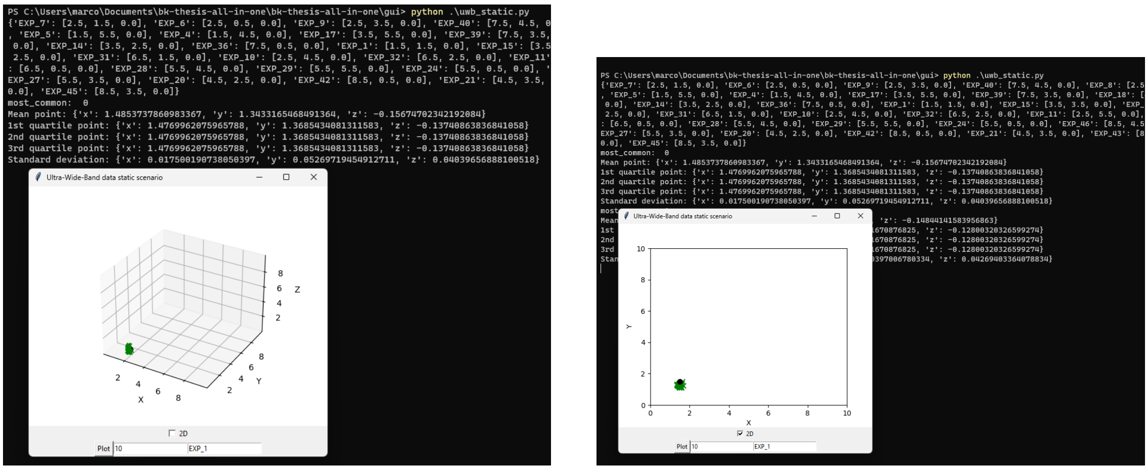

```
PS C:\Users\marco\Documents\bk-thesis-all-in-one\bk-thesis-all-in-one\gui> python .\uwb_static.py
{'EXP_7': [2.5, 1.5, 0.0], 'EXP_6': [2.5, 0.5, 0.0], 'EXP_9': [2.5, 3.5, 0.0], 'EXP_40': [7.5, 4.5, 0
, 'EXP_5': [1.5, 5.5, 0.0], 'EXP_4': [1.5, 4.5, 0.0], 'EXP_17': [3.5, 5.5, 0.0], 'EXP_39': [7.5, 3.5,
 0.0], 'EXP_14': [3.5, 2.5, 0.0], 'EXP_36': [7.5, 0.5, 0.0], 'EXP_1': [1.5, 1.5, 0.0], 'EXP_15': [3.5
 2.5, 0.0], 'EXP_31': [6.5, 1.5, 0.0], 'EXP_10': [2.5, 4.5, 0.0], 'EXP_32': [6.5, 2.5, 0.0], 'EXP_11'
: [6.5, 0.5, 0.0], 'EXP_28': [5.5, 4.5, 0.0], 'EXP_29': [5.5, 5.5, 0.0], 'EXP_24': [5.5, 0.5, 0.0], '
EXP_27': [5.5, 3.5, 0.0], 'EXP_20': [4.5, 2.5, 0.0], 'EXP_42': [8.5, 0.5, 0.0], 'EXP_21': [4.5, 3.5,
0.0], 'EXP_45': [8.5, 3.5, 0.0]}
most_common:  0
Mean point: {'x': 1.4853737860983367, 'y': 1.3433165468491364, 'z': -0.15674702342192084}
1st quartile point: {'x': 1.4769962075965788, 'y': 1.3685434081311583, 'z': -0.13740863836841058}
2nd quartile point: {'x': 1.4769962075965788, 'y': 1.3685434081311583, 'z': -0.13740863836841058}
3rd quartile point: {'x': 1.4769962075965788, 'y': 1.3685434081311583, 'z': -0.13740863836841058}
Standard deviation: {'x': 0.017500190738050397, 'y': 0.05269719454912711, 'z': 0.04039656888100518}
```

(A) 3D Scenario

```
PS C:\Users\marco\Documents\bk-thesis-all-in-one\bk-thesis-all-in-one\gui> python .\uwb_static.py
{'EXP_7': [2.5, 1.5, 0.0], 'EXP_6': [2.5, 0.5, 0.0], 'EXP_9': [2.5, 3.5, 0.0], 'EXP_40': [7.5, 4.5, 0.0], 'EXP_8': [2.5
, 'EXP_5': [1.5, 5.5, 0.0], 'EXP_4': [1.5, 4.5, 0.0], 'EXP_17': [3.5, 5.5, 0.0], 'EXP_39': [7.5, 3.5, 0.0], 'EXP_18': [
 0.0], 'EXP_14': [3.5, 2.5, 0.0], 'EXP_36': [7.5, 0.5, 0.0], 'EXP_1': [1.5, 1.5, 0.0], 'EXP_15': [3.5, 3.5, 0.0], 'EXP_
 2.5, 0.0], 'EXP_31': [6.5, 1.5, 0.0], 'EXP_10': [2.5, 4.5, 0.0], 'EXP_32': [6.5, 2.5, 0.0], 'EXP_11': [2.5, 5.5, 0.0],
: [6.5, 0.5, 0.0], 'EXP_28': [5.5, 4.5, 0.0], 'EXP_29': [5.5, 5.5, 0.0], 'EXP_24': [5.5, 0.5, 0.0], 'EXP_46': [8.5, 4.5
EXP_27': [5.5, 3.5, 0.0], 'EXP_20': [4.5, 2.5, 0.0], 'EXP_42': [8.5, 0.5, 0.0], 'EXP_21': [4.5, 3.5, 0.0], 'EXP_43': [8
0.0], 'EXP_45': [8.5, 3.5, 0.0]}
most_common:  0
Mean point: {'x': 1.4853737860983367, 'y': 1.3433165468491364, 'z': -0.15674702342192084}
1st quartile point: {'x': 1.4769962075965788, 'y': 1.3685434081311583, 'z': -0.13740863836841058}
2nd quartile point: {'x': 1.4769962075965788, 'y': 1.3685434081311583, 'z': -0.13740863836841058}
3rd quartile point: {'x': 1.4769962075965788, 'y': 1.3685434081311583, 'z': -0.13740863836841058}
Standard deviation: {'x': 0.017500190738050397, 'y': 0.05269719454912711, 'z': 0.04039656888100518}
most
Mean                                              , 'z': -0.14844141583956863}
1st                                            670876825, 'z': -0.12800320326599274}
2nd                                            670876825, 'z': -0.12800320326599274}
3rd                                            670876825, 'z': -0.12800320326599274}
Stan                                           397006780334, 'z': 0.04269403364078834}
```

(B) 2D Scenario

FIGURE 7.1: Software that allows to visualize a UWB experiment and allow configure the number of members in a group

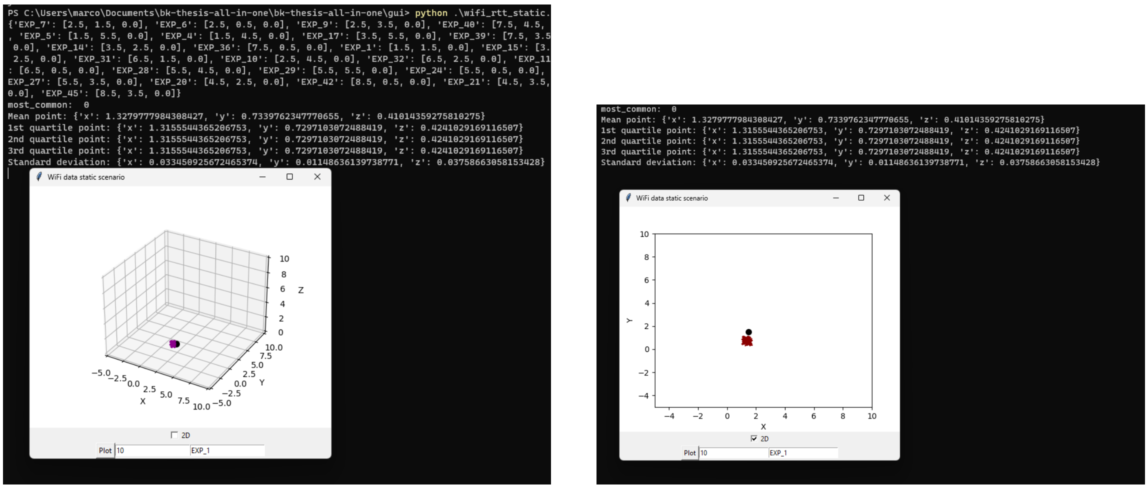

```
PS C:\Users\marco\Documents\bk-thesis-all-in-one\bk-thesis-all-in-one\gui> python .\wifi_rtt_static.
{'EXP_7': [2.5, 1.5, 0.0], 'EXP_6': [2.5, 0.5, 0.0], 'EXP_9': [2.5, 3.5, 0.0], 'EXP_40': [7.5, 4.5,
, 'EXP_5': [1.5, 5.5, 0.0], 'EXP_4': [1.5, 4.5, 0.0], 'EXP_17': [3.5, 5.5, 0.0], 'EXP_39': [7.5, 3.5
 0.0], 'EXP_14': [3.5, 2.5, 0.0], 'EXP_36': [7.5, 0.5, 0.0], 'EXP_1': [1.5, 1.5, 0.0], 'EXP_15': [3.
 2.5, 0.0], 'EXP_31': [6.5, 1.5, 0.0], 'EXP_10': [2.5, 4.5, 0.0], 'EXP_32': [6.5, 2.5, 0.0], 'EXP_11
: [6.5, 0.5, 0.0], 'EXP_28': [5.5, 4.5, 0.0], 'EXP_29': [5.5, 5.5, 0.0], 'EXP_24': [5.5, 0.5, 0.0],
EXP_27': [5.5, 3.5, 0.0], 'EXP_20': [4.5, 2.5, 0.0], 'EXP_42': [8.5, 0.5, 0.0], 'EXP_21': [4.5, 3.5,
0.0], 'EXP_45': [8.5, 3.5, 0.0]}
most_common:  0
Mean point: {'x': 1.3279777984308427, 'y': 0.7339762347770655, 'z': 0.41014359275810275}
1st quartile point: {'x': 1.3155544365206753, 'y': 0.7297103072488419, 'z': 0.4241029169116507}
2nd quartile point: {'x': 1.3155544365206753, 'y': 0.7297103072488419, 'z': 0.4241029169116507}
3rd quartile point: {'x': 1.3155544365206753, 'y': 0.7297103072488419, 'z': 0.4241029169116507}
Standard deviation: {'x': 0.033450925672465374, 'y': 0.011486136139738771, 'z': 0.037586630581534 28}
```

(A) 3D scenario

```
most_common:  0
Mean point: {'x': 1.3279777984308427, 'y': 0.7339762347770655, 'z': 0.41014359275810275}
1st quartile point: {'x': 1.3155544365206753, 'y': 0.7297103072488419, 'z': 0.4241029169116507}
2nd quartile point: {'x': 1.3155544365206753, 'y': 0.7297103072488419, 'z': 0.4241029169116507}
3rd quartile point: {'x': 1.3155544365206753, 'y': 0.7297103072488419, 'z': 0.4241029169116507}
Standard deviation: {'x': 0.033450925672465374, 'y': 0.011486136139738771, 'z': 0.03758663058153428}
```

(B) 2D Scenario

FIGURE 7.2: Software that does visualization of a WiFi RTT experiment and allows configuration of the number of members in a group

Figure 7.3 shows the software module that allows users to visualize dynamic datasets, those with movement. By clicking on the button plot, the subsequent frame is generated, enabling the user to view continuously.

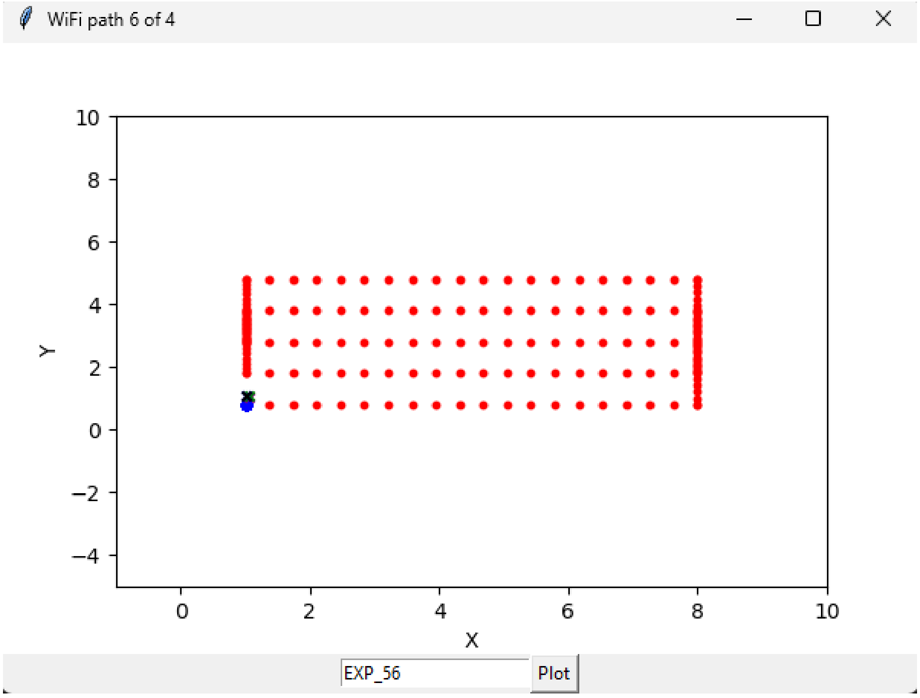

FIGURE 7.3: Software that does visualization of a WiFi RTT/UWB for dynamic experiments

Figure 7.4 illustrates the project structure, which follows a straightforward architecture to improve code readability for future maintenance. The software is organized into individual files, each file typically representing a class, adhering to Object-Oriented Programming (OOP) principles.

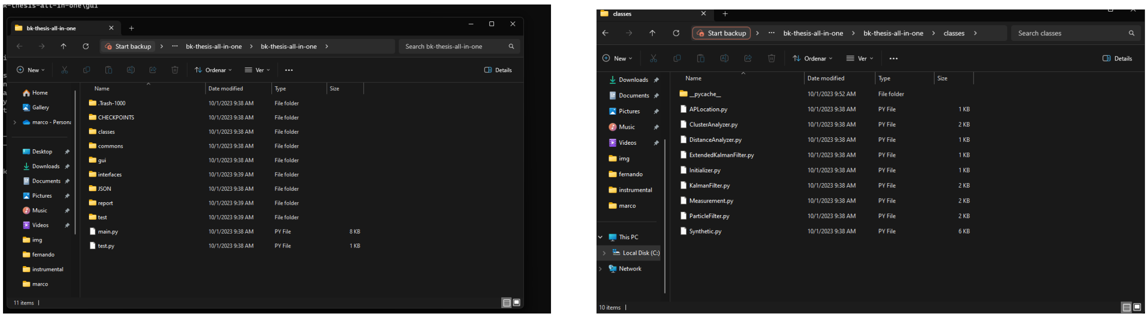

Name	Date modified	Type	Size
.Trash-1000	10/1/2023 9:38 AM	File folder	
CHECKPOINTS	10/1/2023 9:38 AM	File folder	
classes	10/1/2023 9:38 AM	File folder	
commons	10/1/2023 9:38 AM	File folder	
gui	10/1/2023 9:38 AM	File folder	
interfaces	10/1/2023 9:39 AM	File folder	
JSON	10/1/2023 9:38 AM	File folder	
report	10/1/2023 9:39 AM	File folder	
test	10/1/2023 9:39 AM	File folder	
main.py	10/1/2023 9:38 AM	PY File	8 KB
test.py	10/1/2023 9:38 AM	PY File	1 KB

(A) Root Folder

Name	Date modified	Type	Size
__pycache__	10/1/2023 9:52 AM	File folder	
APLocation.py	10/1/2023 9:38 AM	PY File	1 KB
ClusterAnalyzer.py	10/1/2023 9:38 AM	PY File	2 KB
DistanceAnalyzer.py	10/1/2023 9:38 AM	PY File	1 KB
ExtendedKalmanFilter.py	10/1/2023 9:38 AM	PY File	1 KB
Initializer.py	10/1/2023 9:38 AM	PY File	1 KB
KalmanFilter.py	10/1/2023 9:38 AM	PY File	2 KB
Measurement.py	10/1/2023 9:38 AM	PY File	2 KB
ParticleFilter.py	10/1/2023 9:38 AM	PY File	2 KB
Synthetic.py	10/1/2023 9:38 AM	PY File	6 KB

(B) Classes Folder

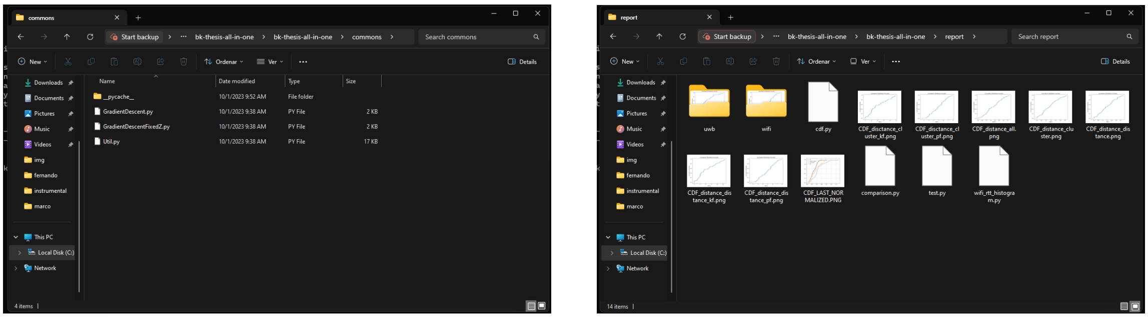

Name	Date modified	Type	Size
__pycache__	10/1/2023 9:52 AM	File folder	
GradientDescent.py	10/1/2023 9:38 AM	PY File	2 KB
GradientDescentFixedZ.py	10/1/2023 9:38 AM	PY File	2 KB
Util.py	10/1/2023 9:38 AM	PY File	17 KB

(C) Commons Folder

uwb
wifi
cdf.py
CDF_disctance_cluster_kf.png
CDF_disctance_cluster_pf.png
CDF_distance_all.png
CDF_distance_cluster.png
CDF_distance_distance.png
CDF_distance_distance_kf.png
CDF_distance_distance_pf.png
CDF_LAST_NORMALIZED.PNG
comparison.py
test.py
wifi_rtt_histogram.py

(D) Report Folder

FIGURE 7.4: Folder Structure of the project

7.4 Final Remarks

As we bring this study to a close, it becomes apparent that the journey begun has been both challenging and rewarding. Our approach to investigating FTM technologies and developing a solution that improves indoor localization accuracy paved the way for a promising future in indoor localization solutions.

The synergistic combination of gradient descent algorithms, clustering techniques, and an adaptable time window strategy has demonstrated significant potential. Furthermore, our research points towards the significant advantages of using redundancy of FTM responders. The correct selection of access points or anchors can be used in conjunction with additional data sources and machine learning approaches to improve the performance of Indoor Positional systems.

However, it is imperative to recognize the challenges faced during the development phase, including the intricate balance between accuracy and computational efficiency. As we navigate these complexities, the road ahead opens up a myriad of opportunities to further refine and enhance the solution.

Bibliography

[1] A. Purnama and M. I. Nashiruddin, "Analysis of microwave communication network planning on ocean topography using space diversity," *Buletin Pos dan Telekomunikasi*, vol. 18, pp. 1–16, 06 2020. [Cited on pages K and 2.]

[2] R. Peng and M. L. Sichitiu, "Angle of arrival localization for wireless sensor networks," in *2006 3rd annual IEEE communications society on sensor and ad hoc communications and networks*, vol. 1. Ieee, 2006, pp. 374–382. [Cited on pages 6 and 12.]

[3] H. Obeidat, W. Shuaieb, O. Obeidat, and R. Abd-Alhameed, "A review of indoor localization techniques and wireless technologies," *Wireless Personal Communications*, vol. 119, pp. 289–327, 2021. [Cited on pages 6, 10, 13, 15, and 16.]

[4] S. Subedi and J.-Y. Pyun, "A survey of smartphone-based indoor positioning system using rf-based wireless technologies," *Sensors*, vol. 20, p. 7230, 12 2020. [Cited on pages K, 7, 9, and 12.]

[5] F. Zafari, A. Gkelias, and K. K. Leung, "A survey of indoor localization systems and technologies," *IEEE Communications Surveys & Tutorials*, vol. 21, no. 3, pp. 2568–2599, 2019. [Cited on pages K, 7, and 8.]

[6] M. Scherhäufl, M. Pichler, D. Müller, A. Ziroff, and A. Stelzer, "Phase-of-arrival-based localization of passive uhf rfid tags," in *2013 IEEE MTT-S International Microwave Symposium Digest (MTT)*, 2013, pp. 1–3. [Cited on page 7.]

[7] J. Joung, S. Jung, S. Chung, and E.-R. Jeong, "Cnn-based tx–rx distance estimation for uwb system localisation," *Electronics Letters*, vol. 55, 08 2019. [Cited on page 8.]

[8] M. Khalaf-Allah, "Particle filtering for three-dimensional tdoa-based positioning using four anchor nodes," *Sensors*, vol. 20, no. 16, 2020. [Online]. Available: https://www.mdpi.com/1424-8220/20/16/4516 [Cited on page 9.]

[9] S. Yiu, M. Dashti, H. Claussen, and F. Perez-Cruz, "Wireless rssi fingerprinting localization," *Signal Processing*, vol. 131, pp. 235–244, 2017. [Cited on pages 10 and 12.]

[10] "UWB Positioning Technology - Strength, Weakness, and How It Works — mapsted.com," https://mapsted.com/blog/uwb-positioning-explained, [Accessed 22-11-2023]. [Cited on page 10.]

[11] L. Team, "An Overview of Ultra-Wideband (UWB) Technology and its Applications — Research Articles — Lumenci — lumenci.com," https://www.lumenci.com/research-articles/ultrawideband, [Accessed 22-11-2023]. [Cited on pages K, 10, and 11.]

[12] G. Shi and Y. Ming, "Survey of indoor positioning systems based on ultra-wideband (uwb) technology," in *Wireless Communications, Networking and Applications: Proceedings of WCNA 2014*. Springer, 2016, pp. 1269–1278. [Cited on page 10.]

[13] M. Elhousni and X. Huang, "A survey on 3d lidar localization for autonomous vehicles," in *2020 IEEE Intelligent Vehicles Symposium (IV)*. IEEE, 2020, pp. 1879–1884. [Cited on page 10.]

[14] "NOAA Office for Coastal Management — coast.noaa.gov," https://coast.noaa.gov/, [Accessed 22-11-2023]. [Cited on pages K and 11.]

[15] Q. Wang, R. Sun, X. Zhang, Y. Sun, and X. lu, "Bluetooth positioning based on weighted k-nearest neighbors and adaptive bandwidth mean shift," *International Journal of Distributed Sensor Networks*, vol. 13, p. 155014771770668, 05 2017. [Cited on pages K and 12.]

[16] "Wi-Fi location: ranging with RTT — Connectivity — Android Developers — developer.android.com," https://developer.android.com/develop/connectivity/wifi/wifi-rtt, [Accessed 21-11-2023]. [Cited on page 13.]

[17] C. Gentner, M. Ulmschneider, I. Kuehner, and A. Dammann, "Wifi-rtt indoor positioning," in *2020 IEEE/ION Position, Location and Navigation Symposium (PLANS)*. IEEE, 2020, pp. 1029–1035. [Cited on page 13.]

[18] "Indoor positioning using time of flight with respect to WiFi access points — people.csail.mit.edu," https://people.csail.mit.edu/bkph/ftmrtt, [Accessed 20-May-2023]. [Cited on page 13.]

[19] I. Martin-Escalona and E. Zola, "Passive round-trip-time positioning in dense ieee 802.11 networks," *Electronics*, vol. 9, p. 1193, 07 2020. [Cited on pages K and 14.]

[20] T. Sanpechuda and L.-o. Kovavisaruch, "A review of rfid localization: Applications and techniques," in *2008 5th international conference on electrical engineering/electronics, computer, telecommunications and information technology*, vol. 2. IEEE, 2008, pp. 769–772. [Cited on page 15.]

[21] J. Armstrong, Y. A. Sekercioglu, and A. Neild, "Visible light positioning: A roadmap for international standardization," *IEEE Communications Magazine*, vol. 51, no. 12, pp. 68–73, 2013. [Cited on pages 15 and 16.]

[22] F. Schill, U. R. Zimmer, and J. Trumpf, "Visible spectrum optical communication and distance sensing for underwater applications," 2004. [Online]. Available: https://api.semanticscholar.org/CorpusID:18170325

[23] T.-H. Do and M. Yoo, "An in-depth survey of visible light communication based positioning systems," *Sensors*, vol. 16, p. 678, 05 2016. [Cited on pages 15 and 16.]

[24] K. Cengiz, "Comprehensive analysis on least-squares lateration for indoor positioning systems," *IEEE Internet of Things Journal*, vol. 8, no. 4, pp. 2842–2856, 2020. [Cited on page 17.]

[25] "Find X location using 3 known (X,Y) location using trilateration — math.stackexchange.com," https://math.stackexchange.com/questions/884807/find-x-location-using-3-known-x-y-location-using-trilateration, [Accessed 27-09-2023]. [Cited on page 17.]

[26] G. Qin, C. Patsakis, and M. Bouroche, "Playing hide and seek with mobile dating applications," vol. 428, 06 2014. [Cited on pages K and 18.]

[27] S. Ruder, "An overview of gradient descent optimization algorithms," *arXiv preprint arXiv:1609.04747*, 2016. [Cited on page 18.]

[28] S. Leelavathy and S. Sophia, "Providing localization using triangulation method in wireless sensor networks," *International journal of innovative technology and exploring engineering*, vol. 4, no. 6, pp. 47–50, 2014. [Cited on page 18.]

[29] “Triangulation maple help,” https://www.maplesoft.com/support/help/maple/view.aspx?path=MathApps%2FTriangulation, [Accessed 27-09-2023]. [Cited on page 18.]

[30] Q. D. Vo and P. De, “A survey of fingerprint-based outdoor localization,” *IEEE Communications Surveys & Tutorials*, vol. 18, no. 1, pp. 491–506, 2015. [Cited on page 19.]

[31] B. Mahesh, “Machine learning algorithms-a review,” *International Journal of Science and Research (IJSR).[Internet]*, vol. 9, no. 1, pp. 381–386, 2020. [Cited on page 19.]

[32] P. Roy and C. Chowdhury, “A survey of machine learning techniques for indoor localization and navigation systems,” *Journal of Intelligent & Robotic Systems*, vol. 101, no. 3, p. 63, 2021. [Cited on page 19.]

[33] “What is supervised learning? — Definition from TechTarget — techtarget.com,” https://www.techtarget.com/searchenterpriseai/definition/supervised-learning, [Accessed 27-09-2023]. [Cited on page 20.]

[34] “Unsupervised Machine learning - Javatpoint — javatpoint.com,” https://www.javatpoint.com/unsupervised-machine-learning, [Accessed 27-09-2023]. [Cited on page 20.]

[35] S. Bhatt, “Reinforcement Learning 101 — towardsdatascience.com,” https://towardsdatascience.com/reinforcement-learning-101-e24b50e1d292, [Accessed 27-09-2023]. [Cited on page 20.]

[36] N. Jain, “An overview of the Gradient Descent algorithm — towardsdatascience.com,” https://towardsdatascience.com/an-overview-of-the-gradient-descent-algorithm-8645c9e4de1e, [Accessed 27-09-2023]. [Cited on page 20.]

[37] Crypto1, “How Does the Gradient Descent Algorithm Work in Machine Learning? — analyticsvidhya.com,” https://www.analyticsvidhya.com/blog/2020/10/how-does-the-gradient-descent-algorithm-work-in-machine-learning/, [Accessed 27-09-2023]. [Cited on page 20.]

[38] Q. Li, R. Li, K. Ji, and W. Dai, “Kalman filter and its application,” in *2015 8th International Conference on Intelligent Networks and Intelligent Systems (ICINIS)*. IEEE, 2015, pp. 74–77. [Cited on page 21.]

[39] V. Stojanovic and N. Nedic, “Robust kalman filtering for nonlinear multivariable stochastic systems in the presence of non-gaussian noise,” *International Journal of Robust and Nonlinear Control*, vol. 26, no. 3, pp. 445–460, 2016. [Cited on page 21.]

[40] W. Franklin, “Kalman Filter Explained Simply - The Kalman Filter — thekalmanfilter.com,” https://thekalmanfilter.com/kalman-filter-explained-simply/, [Accessed 27-09-2023]. [Cited on page 21.]

[41] Y. Boers and J. N. Driessen, “Particle filter based detection for tracking,” in *Proceedings of the 2001 American Control Conference.(Cat. No. 01CH37148)*, vol. 6. IEEE, 2001, pp. 4393–4397. [Cited on page 22.]

[42] “Particle Filters: A Hands-On Tutorial — ncbi.nlm.nih.gov,” https://www.ncbi.nlm.nih.gov/pmc/articles/PMC7826670/, [Accessed 27-09-2023]. [Cited on page 23.]

[43] “Introduction to Estimation Filters - MATLAB & Simulink - MathWorks,” https://jp.mathworks.com/help/fusion/ug/introduction-to-estimation-filters.html, [Accessed 23-11-2023]. [Cited on pages K and 24.]

[44] “Multipath Propagation - an overview — ScienceDirect Topics — sciencedirect.com,” https://www.sciencedirect.com/topics/engineering/multipath-propagation, [Accessed 27-09-2023]. [Cited on page 24.]

[45] “Signal fading: Causes, effects, and mitigation techniques — huawei.com,” https://forum.huawei.com/enterprise/en/signal-fading-causes-effects-and-mitigation-techniques/thread/683845701034983424-667213872962088960, [Accessed 27-09-2023]. [Cited on pages K and 25.]

[46] D. B. Faria *et al.*, “Modeling signal attenuation in ieee 802.11 wireless lans-vol. 1,” *Computer Science Department, Stanford University*, vol. 1, 2005. [Cited on page 26.]

[47] “Non-line-of-sight imaging - Nature Reviews Physics — nature.com,” https://www.nature.com/articles/s42254-020-0174-8, [Accessed 27-09-2023]. [Cited on page 27.]

[48] P. Bahl and V. N. Padmanabhan, “Radar: An in-building rf-based user location and tracking system,” in *Proceedings IEEE INFOCOM 2000. Conference on computer communications. Nineteenth annual joint conference of the IEEE computer and communications societies (Cat. No. 00CH37064)*, vol. 2. Ieee, 2000, pp. 775–784. [Cited on page 29.]

[49] İ. Güvenc, "Enhancements to rss based indoor tracking systems using kalman filters," Ph.D. dissertation, Citeseer, 2003. [Cited on page 29.]

[50] D. Vasisht, S. Kumar, and D. Katabi, "{Decimeter-Level} localization with a single {WiFi} access point," in *13th USENIX symposium on networked systems design and implementation (NSDI 16)*, 2016, pp. 165–178. [Cited on pages 29 and 32.]

[51] M. Kotaru, K. Joshi, D. Bharadia, and S. Katti, "Spotfi: Decimeter level localization using wifi," in *Proceedings of the 2015 ACM conference on special interest group on data communication*, 2015, pp. 269–282. [Cited on page 30.]

[52] J. Xiong and K. Jamieson, "{ArrayTrack}: A {Fine-Grained} indoor location system," in *10th USENIX Symposium on Networked Systems Design and Implementation (NSDI 13)*, 2013, pp. 71–84. [Cited on page 31.]

[53] R. Schmidt, "Multiple emitter location and signal parameter estimation," *IEEE transactions on antennas and propagation*, vol. 34, no. 3, pp. 276–280, 1986. [Cited on page 31.]

[54] J. Gjengset, J. Xiong, G. McPhillips, and K. Jamieson, "Phaser: Enabling phased array signal processing on commodity wifi access points," in *Proceedings of the 20th annual international conference on Mobile computing and networking*, 2014, pp. 153–164. [Cited on page 31.]

[55] J. Xiong, K. Sundaresan, and K. Jamieson, "Tonetrack: Leveraging frequency-agile radios for time-based indoor wireless localization," in *Proceedings of the 21st Annual International Conference on Mobile Computing and Networking*, 2015, pp. 537–549. [Cited on pages 31 and 32.]

[56] X. Wang, L. Gao, S. Mao, and S. Pandey, "Csi-based fingerprinting for indoor localization: A deep learning approach," *IEEE transactions on vehicular technology*, vol. 66, no. 1, pp. 763–776, 2016. [Cited on page 32.]

[57] C. Luo, L. Cheng, M. C. Chan, Y. Gu, J. Li, and Z. Ming, "Pallas: Self-bootstrapping fine-grained passive indoor localization using wifi monitors," *IEEE Transactions on Mobile Computing*, vol. 16, no. 2, pp. 466–481, 2016. [Cited on page 32.]

[58] S. Krishnan, P. Sharma, Z. Guoping, and O. H. Woon, "A uwb based localization system for indoor robot navigation," in *2007 IEEE International Conference on Ultra-Wideband*. IEEE, 2007, pp. 77–82. [Cited on page 33.]

[59] J. Shen and A. F. Molisch, "Passive location estimation using toa measurements," in *2011 IEEE International Conference on Ultra-Wideband (ICUWB)*. IEEE, 2011, pp. 253–257. [Cited on page 33.]

[60] J. Xu, M. Ma, and C. L. Law, "Position estimation using uwb tdoa measurements," in *2006 IEEE International Conference on Ultra-Wideband*. IEEE, 2006, pp. 605–610. [Cited on page 33.]

[61] A. Mandal, C. V. Lopes, T. Givargis, A. Haghighat, R. Jurdak, and P. Baldi, "Beep: 3d indoor positioning using audible sound," in *Second IEEE Consumer Communications and Networking Conference, 2005. CCNC. 2005*. IEEE, 2005, pp. 348–353. [Cited on page 33.]

[62] C. Peng, G. Shen, Y. Zhang, Y. Li, and K. Tan, "Beepbeep: a high accuracy acoustic ranging system using cots mobile devices," in *Proceedings of the 5th international conference on Embedded networked sensor systems*, 2007, pp. 1–14. [Cited on page 34.]

[63] G.-y. Jin, X.-y. Lu, and M.-S. Park, "An indoor localization mechanism using active rfid tag," in *IEEE International Conference on Sensor Networks, Ubiquitous, and Trustworthy Computing (SUTC'06)*, vol. 1. IEEE, 2006, pp. 4–pp. [Cited on page 34.]

[64] J. Wang, F. Adib, R. Knepper, D. Katabi, and D. Rus, "Rf-compass: Robot object manipulation using rfids," in *Proceedings of the 19th annual international conference on Mobile computing & networking*, 2013, pp. 3–14. [Cited on page 35.]

[65] J. Wang and D. Katabi, "Dude, where's my card? rfid positioning that works with multipath and non-line of sight," in *Proceedings of the ACM SIGCOMM 2013 conference on SIGCOMM*, 2013, pp. 51–62. [Cited on page 35.]

[66] F. J. Gonzalez-Castano and J. García-Reinoso, "Bluetooth location networks," in *Global Telecommunications Conference, 2002. GLOBECOM'02. IEEE*, vol. 1. IEEE, 2002, pp. 233–237. [Cited on page 36.]

[67] R. Bruno and F. Delmastro, “Design and analysis of a bluetooth-based indoor localization system,” in *IFIP International Conference on Personal Wireless Communications*. Springer, 2003, pp. 711–725. [Cited on page 36.]

[68] J. J. Diaz, R. d. A. Maues, R. B. Soares, E. F. Nakamura, and C. M. Figueiredo, “Bluepass: An indoor bluetooth-based localization system for mobile applications,” in *The IEEE symposium on Computers and Communications*. IEEE, 2010, pp. 778–783. [Cited on page 37.]

[69] F. Faheem, “Ibeacon based proximity and indoor localization system,” 2016. [Cited on page 37.]

[70] R. Ayyalasomayajula, D. Vasisht, and D. Bharadia, “Bloc: Csi-based accurate localization for ble tags,” in *Proceedings of the 14th International Conference on emerging Networking EXperiments and Technologies*, 2018, pp. 126–138. [Cited on page 37.]

[71] B. Islam, M. Uddin, S. Mukherjee, and S. Nirjon, “Rethinking ranging of unmodified ble peripherals in smart city infrastructure,” in *Proceedings of the 9th ACM Multimedia Systems Conference*, 2018, pp. 339–350. [Cited on page 37.]

[72] I. A. Ashokaraj, P. M. Silson, A. Tsourdos, and B. A. White, “Robust sensor-based navigation for mobile robots,” *IEEE Transactions on Instrumentation and Measurement*, vol. 58, no. 3, pp. 551–556, 2008. [Cited on page 38.]

[73] M. Kieffer, L. Jaulin, É. Walter, and D. Meizel, “Robust autonomous robot localization using interval analysis,” *Reliable computing*, vol. 6, no. 3, pp. 337–362, 2000. [Cited on page 38.]

[74] F. Gustafsson, F. Gunnarsson, N. Bergman, U. Forssell, J. Jansson, R. Karlsson, and P.-J. Nordlund, “Particle filters for positioning, navigation, and tracking,” *IEEE Transactions on signal processing*, vol. 50, no. 2, pp. 425–437, 2002. [Cited on page 38.]

[75] F. Gustafsson, “Particle filter theory and practice with positioning applications,” *IEEE Aerospace and Electronic Systems Magazine*, vol. 25, no. 7, pp. 53–82, 2010.

[76] M. S. Arulampalam, S. Maskell, N. Gordon, and T. Clapp, “A tutorial on particle filters for online nonlinear/non-gaussian bayesian tracking,” *IEEE Transactions on signal processing*, vol. 50, no. 2, pp. 174–188, 2002. [Cited on page 38.]

[77] A. Ward, A. Jones, and A. Hopper, "A new location technique for the active office," *IEEE Personal communications*, vol. 4, no. 5, pp. 42–47, 1997. [Cited on page 38.]

[78] R. K. Harle and A. Hopper, "Deploying and evaluating a location-aware system," in *Proceedings of the 3rd international conference on Mobile systems, applications, and services*, 2005, pp. 219–232. [Cited on page 38.]

[79] J. Xiong, "Pushing the limits of indoor localization in today's wi-fi networks," Ph.D. dissertation, UCL (University College London), 2015. [Cited on page 38.]

[80] N. B. Priyantha, A. Chakraborty, and H. Balakrishnan, "The cricket location-support system," in *Proceedings of the 6th annual international conference on Mobile computing and networking*, 2000, pp. 32–43. [Cited on page 38.]

[81] E. Di Lascio, A. Varshney, T. Voigt, and C. Pérez-Penichet, "Localight-a battery-free passive localization system using visible light," in *2016 15th ACM/IEEE International Conference on Information Processing in Sensor Networks (IPSN)*. IEEE, 2016, pp. 1–2. [Cited on page 39.]

[82] V. B. Vales, O. C. Fernández, T. Domínguez-Bolaño, C. J. Escudero, and J. A. García-Naya, "Fine time measurement for the internet of things: a practical approach using esp32," *IEEE Internet of Things Journal*, vol. 9, no. 19, pp. 18 305–18 318, 2022. [Cited on page 41.]